The impact of extracellular matrix on the precision medicine utility of pancreatic cancer patient-derived organoids

Jan C. Lumibao[1], Shira R. Okhovat[1], Kristina L. Peck[1], Xiaoxue Lin[1], Kathryn Lande[1], Jingjing Zou[2*], Dannielle D. Engle[1*]

[1]Salk Institute for Biological Studies, [2]University of California San Diego

Keywords: organoids, PDAC, pharmacotyping, precision medicine, basement membrane extract

*Co-corresponding authors

Corresponding authors:
Dannielle D. Engle, Ph.D.
Salk Institute for Biological Studies
10010 N. Torrey Pines Rd.
La Jolla, CA 92037
Phone: (858) 453-4100 X1312
E-mail: engle@salk.edu

Jingjing Zou, Ph.D.
Division of Biostatistics and Bioinformatics
Herbert Wertheim School of Public Health and Human Longevity Science
University of California San Diego
3855 Health Sciences Drive Ste. 3035
La Jolla, CA 92093-0901
Phone: (858) 822-4818
E-mail: j2zou@ucsd.edu

Conflict of interest: The authors have declared that no conflict of interest exists

Word count: 4688
Main Figures: 4
Supplementary Figures: 9
Supplementary Tables: 2

Abstract

The use of patient-derived organoids (PDOs) to characterize therapeutic sensitivity and resistance (pharmacotyping) is a promising precision medicine approach. The potential of this approach to inform clinical decisions is now being tested in several large multi-institutional clinical trials. PDOs are cultivated in extracellular matrix from basement membrane extracts (BMEs) that are most commonly acquired commercially. Each clinical site utilizes distinct BME lots and may be restricted due to the availability of commercial BME sources. However, the impact of different sources and lots of BMEs on organoid drug response is unknown. Here, we tested the impact of BME source and lot on proliferation, chemotherapy and targeted therapy drug response, and gene expression in mouse and human pancreatic ductal adenocarcinoma (PDA) organoids. Both human and mouse organoids displayed increased proliferation in Matrigel (Corning) compared to Cultrex (RnD) and UltiMatrix (RnD). However, we observed no substantial impact on drug response when oragnoids were cultured in Matrigel, Cultrex, or UltiMatrix. We also did not observe major shifts in gene expression across the different BME sources, and PDOs maintained their Classical or Basal-like designation. Overall, we find that BME source (Matrigel, Cultrex, UltiMatrix) does not shift PDO dose-response curves and drug testing results, indicating that PDO pharmacotyping is a robust approach for precision medicine.

Introduction

The 5-year relative survival rate for patients with pancreatic ductal adenocarcinoma (PDA) is 12% (*1*). As the incidence of PDA continues to rise (*2*), strategies to increase survival are imperative. Surgical resection remains the only curative option. However, most patients are ineligible due to the presence of metastasis at the time of diagnosis (*3*). Standard-of-care chemotherapeutic regimens include gemcitabine/nab-paclitaxel and FOLFIRINOX, which demonstrate median survival times of 8.5 and 11.1 months, respectively (*4, 5*). Further, as heterogeneity in tumor biology and treatment response continues to be revealed, personalized medicine approaches are becoming increasingly necessary.

The use of patient-derived organoids (PDOs) has the potential to revolutionize care for patients with PDA (*6*). PDOs are 3D cultures in defined conditions that support propagation of normal, premalignant, and neoplastic cells from primary tissue (*7-11*). Organoid technology has emerged as a promising avenue for precision medicine (*12*). The ability to derive PDA PDOs from surgical resections, rapid autopsies (RAP), and endoscopic ultrasound guided fine needle biopsies allows for a broad sampling of patients with PDA to encompass inter- and intra-patient tumor heterogeneity (*8*). Importantly, PDA PDOs mirror patient tumor genetics, gene expression, and treatment response, situating them as a promising tool for more precision medicine efforts to identify alternative treatment strategies (*8, 13-15*).

As the use of organoids has expanded and become more accessible, variations in culture conditions have been introduced to optimize PDA PDO generation and growth. A number of studies have delineated the impact of the liquid media composition on organoid phenotype, transcriptome, and drug response (*16, 17*). Commercial products to support organoid studies have become more widespread, including a wide variety of basement membrane extracts (BME), which serve as 3D scaffolds. Recent studies have described the use of fully synthetic and defined hydrogels to support organoids of colon, bile duct, and mammary gland origin (*18-21*). However, BMEs derived from Engelbreth-Holm-Swarm (EHS) murine sarcomas, most notably Matrigel

27 (Corning), but also products such as Cultrex and UltiMatrix (RnD), remain the most widely used
28 (*19*). EHS-tumor-derived BMEs contain heterogenous mixtures of extracellular matrix proteins,
29 primarily laminins, collagen IV, entactin, and perlecan, as well as tumor-derived proteins and
30 growth factors, which contribute to batch-to-batch variability (*18, 19*). Regardless, these BMEs
31 have historically served as the scaffold for organoid culture. However, the impact of different EHS-
32 tumor-derived BMEs on organoid growth, chemosensitivity, and global gene expression remains
33 unclear. Importantly, previous reports have demonstrated the clinical utility and relevance of PDA
34 PDO pharmacotyping using Matrigel (*8, 13, 15*). These studies and others have prompted the
35 design of clinical trials based on the use of organoid-guided chemotherapy. However, due to the
36 CoVID-19 pandemic, severe supply chain issues have limited BME availability. These issues
37 range from complete inability to secure the same commercial source of BME or dramatic reduction
38 of available BME within the same lot. The impact of the commercial source and lot of BME on
39 drug response and prognostic gene expression programs has not been explored, yet is critical for
40 the deployment of PDO clinical trials.

41 Here, we report the impact of BME on PDA organoid growth, response to standard-of-care
42 chemotherapy as well as targeted therapy, and gene expression patterns. While we find that BME
43 source has a significant and substantial impact on organoid growth, drug response and gene
44 expression remain consistent across multiple lots and commercial sources. Results from this
45 study provide insights into selecting BME for organoid culture and for characterizing PDO
46 sensitivity and resistance to both chemotherapies and targeted therapies, which may assist in
47 guiding clinical decisions.

48

49 **Results**

50 *BME impacts mouse and human organoid growth*

51 To investigate the influence of BME on organoid growth, human and mouse PDA
52 organoids (**Supplementary Table 1-2**) were cultivated in Matrigel 04 (lot #1062004) and then

53 plated in either Matrigel 04, Matrigel 01 (lot #0287001), Cultrex 83 (lot #1564183), Cultrex 87 (lot
54 #1586187), or UltiMatrix 96 (lot #1637796). Intracellular ATP levels were measured after 4
55 (mouse) or 6 days of culture (human). Human PDOs and mouse organoids exhibited reduced
56 growth in Cultrex and UltiMatrix compared to Matrigel (**Figure 1A-B, Supplementary Figure 2**).
57 Mouse organoid proliferation did not recover even after multiple passages in Cultrex, suggesting
58 that this growth deficit is not due to a lack of adaptation period (data not shown). In most
59 experimental replicates across mouse and human organoids, there was no difference in
60 proliferation between Matrigel lots. In 1 out of 3 experiments, there was a small but significant
61 decrease (<10%) in growth of hM1F and hF24 in Matrigel 01 compared to Matrigel 04
62 (**Supplementary Figure 2A-B**). Similarly, 1 out of 2 experiments demonstrated a significant
63 decrease (24%) in hT1 growth in Matrigel 01 (**Supplementary Figure 2C**). Mouse organoid
64 mT69B consistently exhibited no significant differences in intracellular ATP levels between
65 Matrigel lots (n=4/4), while mT69A exhibited 17-23% changes between Matrigel lots (n=2/4)
66 (**Supplementary Figure 2D-E**). In nearly all hPDO experiments, there was a significant, and
67 sometimes substantial (e.g., 27% in Cultrex 83 relative to Matrigel 04), reduction in growth when
68 cultured in either lot of Cultrex or UltiMatrix compared to Matrigel 04 (**Figure 1A, Supplementary**
69 **Figure 2A-B**). Mouse organoids exhibited more mixed results across experimental repeats, but
70 consistently (n=3/4 mT69A, n=4/4 mT69B) exhibited significant, and sometimes substantial (e.g.,
71 55% decrease in Ultimatrix 96 relative to Matrigel 04), decreased growth in UltiMatrix 96 (**Figure**
72 **1B, Supplementary Figure 2D-E**). In the setting of Cultrex, mouse organoid proliferation trended
73 slower relative to Matrigel. mT69A and B grew significantly slower in Cultrex 83 (A: n=2/4, B: 2/4)
74 and 87 (A: n=3/4, B: 2/4), while exhibiting no significant difference relative to Matrigel 04 in 25-
75 50% of the experiments. These data collectively indicate that mouse and human organoids grow
76 significantly more in Matrigel compared to Cultrex or UltiMatrix. The impact of BME source on
77 PDO expansion may be potentially problematic for completion of drug testing for patients within
78 a clinically relevant timeline.

79

80 *BME has minimal impact on drug response*

81 To investigate the influence of BME on drug response, we measured the dose-response
82 of both mouse and human organoids to standard-of-care chemotherapies: gemcitabine,
83 paclitaxel, SN-38 (active metabolite of irinotecan), oxaliplatin, and 5-fluorouracil (5-FU), as well
84 as the targeted small molecule trametinib (third generation MEKi) (**Supplementary Figure 1**).
85 Organoids were allowed to reform and then subjected to pharmacotyping. We found that the dose-
86 response curves for gemcitabine, SN-38, and trametinib across all BMEs were largely overlapping
87 in both hF24 and hM1F (n=3/3) (**Figure 1C-D**, **Supplementary Figure 3A-B**). The dose response
88 curves in hT1 were also consistent across BMEs for SN-38 (n=2/2), but exhibited some variability
89 for gemcitabine (n=1/2) and trametinib (n=1/2) between Matrigel, Cultrex, and Ultimatrix
90 **(Supplementary Figure 3C**)**.** Paclitaxel dose-response curves across all BMEs were also largely
91 overlapping in hM1F (n=3/3) (**Figure 1D**), hT1 (n=2/2) **(Supplementary Figure 3C**)**,** and hF24
92 (n=2/3) (**Figure 1C, Supplementary Figure 3A).** Oxaliplatin also displayed consistent dose-
93 response curves regardless of BME hF24 (n=3/3), hM1F (n=2/3), and hT1 (n=2/2) (**Figure 1C-D**,
94 **Supplementary Figure 3A-C**). Additionally, 5-FU exhibited overlapping dose-response curves in
95 hF24 (n=3/3) (**Figure 1C**, **Supplementary Figure 3A**) and hM1F (n=2/3) (**Figure 1D**,
96 **Supplementary Figure 3B**). However, we observed more variability in dose-response curves for
97 5-FU in hT1 as a function of BME in both experimental repeats conducted (**Supplementary**
98 **Figure 3C**).

99 Mouse organoids were less sensitive to all agents tested relative to hPDOs, with
100 oxaliplatin and 5-FU dose-response curves failing to reach 50% cytotoxicity (**Supplementary**
101 **Figure 3D-E**). Gemcitabine and SN-38 mouse organoid dose response curves exhibited no
102 consistent or substantial shifts when cultured in different BMEs (**Supplementary Figure 3D-E**).
103 Dose-response curves for trametinib were also largely overlapping regardless of BME for both
104 mT69A (n=3/4) and mT69B (n=3/4), although both organoid lines were more resistant in 1 out of

105 4 experimental replicates when cultured in UltiMatrix 96 (**Supplementary Figure 3D-E**). We
106 observed a similar dose response shift for paclitaxel when mouse organoids were cultured in
107 Ultimatrix (n=1/4) (**Supplementary Figure 3D-E**). Overall, these data demonstrate that choice of
108 BME does not induce consistent shifts in dose-response curves for PDOs treated with standard-
109 of-care chemotherapies or trametinib, suggesting that either Matrigel, Cultrex, or UltiMatrix would
110 be appropriate for PDO pharmacotyping analyses.
111
112 *BME does not induce significant alterations in dose-response parameters*
113 We next compared dose-response parameters to gain further insight into subtle changes
114 in dose response curves both within individual experiments and across all experimental replicates.
115 Within each individual experimental replicate, we performed statistical analyses to identify
116 differences in the half maximum inhibitory concentration (IC50s), Hill slope, area under the curve
117 (AUC), and standard deviation of the residuals (Sy.x) between BME lots and sources (*22*).
118 We observed a modest number of instances in which IC50s were statistically significant
119 between BMEs within experimental replicates (**Figure 2A-B, Supplementary Figure 4**).
120 Significant pairwise comparisons in IC50 were predominantly observed between Matrigel and
121 Cultrex or between Matrigel and UltiMatrix. Across all organoids, drug treatments, and BME
122 comparisons, statistical differences between lots of Matrigel (04 vs 01) were observed only once
123 in a single experimental replicate (Paclitaxel, hF24) (**Supplementary Figure 4A**). Similarly,
124 statistical differences between lots of Cultrex (83 vs 87) were observed in only two experimental
125 replicate (SN-38, hM1F; 5-FU, mT69A) (**Supplementary Figure 4B**). These data indicate that lot
126 within the same BME source has little impact on drug IC50. Differences in IC50s for oxaliplatin
127 and trametinib were rarely significant, occurring in 1/16 experiments (hT1, Matrigel 04 vs. Cultrex
128 87) (**Supplementary Figure 4C**) and 2/16 experiments (hM1F, Matrigel 01 vs. UltiMatrix; mT69A,
129 Matrigel 01 vs. UltiMatrix, Cultrex 87, Cultrex 83 vs. UltiMatrix) (**Supplementary Figure 4B, D**),
130 respectively. Conversely, we consistently observed statistical differences in gemcitabine IC50

131 between Matrigel and Cultrex/UltiMatrix in each experimental replicate of hF24 and hM1F (**Figure**
132 **2**, **Supplementary Figure 4A-B**), as well as in hT1 (n=1/2), mT69A (n=1/4), and mT69B (n=2/4)
133 (**Supplementary Figure 4C-E**). Statistical differences in paclitaxel IC50 were observed in hF24
134 (n=1/3), hM1F (n=1/3), hT1 (n=2/2), and mT69B (n=1/4) (**Supplementary Figure 4A-C, E**).
135 Lastly, differences in 5-FU IC50 were observed in only one experimental replicate for hF24,
136 mT69A, and mT69B (**Figure 2A**, **Suppelementary Figure 4D-E**). To further compare differences
137 in dose-response across experimental repeats, we calculated average IC50 concentrations
138 (**Figure 2C-D**, **Supplementary Figure 6**). For all hPDOs, we observed no statistically significant
139 alterations in mean IC50s over experimental repeats calculated for any drug as a function of BME
140 (**Figure 2C-D**, **Supplementary Figure 6A**). Similarly, mouse organoids exhibited no statistically
141 significant shifts in drug IC50, regardless of which BME organoids were plated in (**Supplementary**
142 **Figure 6B-C**).

143 Hill slope is another metric of drug potency that has been suggested to offer higher
144 predictive power than IC50 (*23*). Pairwise comparisons of Hill slope revealed little to no significant
145 differences among BMEs on a per-drug or per-organoid basis (**Supplementary Figure 5**). The
146 only instances in which Hill slopes were statistically distinct between BMEs were in mouse
147 organoids treated with 5-FU, likely due to the resistant nature of these organoids to 5-FU yielding
148 disparate dose-response curves (**Supplementary Figure 5D-E**).

149 We also rarely observed changes in average dose-response curve AUCs across BMEs.
150 Between BME lot, there were not significant AUC differences. AUCs for hF24 treated with
151 paclitaxel were slightly (1.28- to 1.3-fold) but significantly higher in Cultrex 83 or Cultrex 87
152 compared to Matrigel 04 (**Figure 2E**). Similarly, calculated AUCs for hM1F treated with
153 gemcitabine were 1.3-fold higher on average in Cultrex 83 compared to Matrigel 04 (**Figure 2F**).
154 Lastly, AUCs for mT69A treated with paclitaxel were increased in Ultimatrix 96 compared to
155 Matrigel 04 (1.28-fold) (**Supplementary Figure 7B**). In all other mouse and human drug-organoid
156 combinations tested, there were not significant differences in mean AUC across multiple

157 experiments. These data suggest that while minimal differences in drug response exist, the most
158 rigorous approach is to complete pharmacotyping analyses using the same commercial BME
159 source.

160 We next sought to analyze dose-response curve goodness-of-fit as a parameter of plating
161 consistency in each BME within and across experimental replicates. We measured Sy.x as an
162 estimate of goodness-of-fit. In general, higher Sy.x values indicate larger deviations of data points
163 from the fit regression curve. Sy.x values for Cultrex 83 were relatively consistent across
164 experimental replicates, with low absolute values (<10%) and low inter-experimental variability
165 (**Figure 3A-B**). The largest variations in Sy.x across experimental replicates in Cultrex were hF24
166 treated with SN-38 and 5-FU, and hM1F treated with gemcitabine and oxaliplatin (**Figure 3A-B**).
167 Sy.x values were larger on average for Cultrex 83 in hM1F treated with oxaliplatin (mean =
168 20.37%). Cultrex 87 performed consistently as well (ranging from 1.6 – 11.5%), with the most
169 statistical variance across experiments observed in hF24 treated with gemcitabine (**Figure 3A**).
170 UltiMatrix 96, relative to the other BMEs, exhibited higher experimental variability in Sy.x values,
171 with greater variance observed in hF24 treated with gemcitabine (4.1 – 11%) and oxaliplatin (7.6
172 – 22.3%); and hM1F treated with gemcitabine (4.0 – 15.8%), paclitaxel (4.6 – 14.1%), oxaliplatin
173 (7.5 – 26%), and trametinib (4.8 – 12.6%) (**Figure 3A-B**). Matrigel 04 yielded consistent and
174 relatively low Sy.x values (<10%) across all experimental replicates, with the exception of hF24
175 treated with 5-FU (6.3 – 13.3%) (**Figure 3A**). Similarly, Matrigel 01 demonstrated low and
176 consistent Sy.x values across treatments, experimental replicates, and hPDOs tested, as
177 evidenced by low standard deviations and low Sy.x absolute values **(Figure 3A, Supplementary**
178 **Figure 8**). Overall, these results indicate better dose-response curve goodness-of-fit from
179 experiment to experiment when human organoids are cultured in Matrigel.

180 For mouse organoids, similar trends were observed, albeit with higher absolute Sy.x
181 values across almost all conditions (range: 4.5 – 40.8%) (**Figure 3C-D**). In general, mouse
182 organoids are more sensitive to single cell dissociation protocols and have higher growth rates,

183 both of which contribute to increased variance and necessitate shorter pharmacotyping
184 experimental time courses (3 days for mouse organoids vs 5 days for hPDOs). Over the course
185 of 4 experimental replicates, UltiMatrix 96 demonstrated a high degree of statistical variability in
186 Sy.x values relative to the other BMEs tested, notably for mT69A treated with paclitaxel (9.0 -
187 24.1%) and oxaliplatin (13.5 - 23.9%), and mT69B treated with gemcitabine (8.81 - 19.8%)
188 (**Figure 3C-D**). Relative to the other BMEs tested, Cultrex lots also exhibited high levels of
189 variability in Sy.x. Cultrex 83 exhibited a high degree of variability for mT69A treated with 5-FU
190 (7.7 - 22.7%) and trametinib (5.9 - 14.7%), and mT69B treated with paclitaxel (6.3 - 17.1%) and
191 SN-38 (7.3 - 40.8%) (**Figure 3C-D**). Similar variability in Sy.x across experimental replicates was
192 observed for Cultrex 87 in mT69A treated with oxaliplatin (11.7 - 26.8%) and 5-FU (12.2 - 30.5%),
193 and mT69B treated with gemcitabine (6.9 - 19.4%), paclitaxel (7.9 - 23.6%), and trametinib (8.2 -
194 39.9%) (**Figure 3C-D**). Sy.x values were consistent for mT69B treated with paclitaxel when
195 cultured in Ultimatrix 96 (10.7 - 10.9%) (**Figure 3D**). Both Matrigel 04 and Matrigel 01 showed
196 relatively consistent Sy.x values in the mouse organoid context but exhibited some biological and
197 experimental variance. Most notably, mT69A and mT69B are relatively resistant to oxaliplatin and
198 5-FU and exhibited relatively high Sy.x absolute values (20-30%) in these conditions compared
199 other drug treatments (**Figure 3C-D**).

200 Overall, we observed no statistically significant differences in average Sy.x values for both
201 human and mouse organoids across BMEs and all drugs (**Figure 3, Supplementary Figure 8**).
202 However, for both human and mouse organoids, both lots of Matrigel exhibited more consistent
203 Sy.x values across experimental replicates compared to Cultrex or UltiMatrix, as evidenced by
204 lower variance in Sy.x values across experiments (**Figure 3**). Lot-to-lot variability was more
205 pronounced for Cultrex compared to Matrigel for both human and mouse organoids. Collectively,
206 these data indicate that drug dose-response curve fitting is stable across the BMEs tested.

207

208 *Gene expression and organoid subtype classification are not influenced by BME*

209 Although we did not observe substantial shifts in drug response as a function of BME lot
210 or source, alterations in intracellular signaling and cell state represented another potential variable
211 influenced by BME composition. Therefore, we also investigated BME induced changes in gene
212 expression or PDA subtype classification (*24*). To this end, mouse organoids (mT69A, mT69B,
213 mT9) and human PDOs (hF24, hM1F, hT1) were each cultured in each BME (Matrigel 04, Matrigel
214 01, Cultrex 83, Cultrex 87, and Ultimatrix 96) for 3 days and subjected to RNA-seq analyses
215 (**Supplementary Figure 1**). Multivariate analysis of resultant Z-scores of organoid normalized
216 counts indicated that both mouse and human samples clustered well based on organoid line
217 (**Figure 4A**, **Supplementary Figure 9C-D**). However, samples did not cluster significantly based
218 on BME (**Figure 4A, Supplementary Figure 9C-D, F-G**). Gene expression was largely
219 unchanged between Matrigel lots in both human and mouse organoids (0-2 differentially
220 expressed genes, 20 in hM1F) (**Supplementary Figure 9A-B**). Similarly, minimal gene
221 expression changes were observed in human and mouse organoids between Cultrex lots (0-4
222 differentially expressed genes) (**Supplementary Figure 9A-B**). Between BME sources, we
223 observed more changes in gene expression, but these were not consistent between organoid
224 lines. For example, hT1 (Stage 2B) displayed 522 differentially expressed genes between Matrigel
225 04 and UltiMatrix, whereas hF24 (Stage 4) and hM1F (Stage 4, lung metastasis) presented 0
226 (**Supplementary Figure 9A**). Similarly, mT69B (KPC PDA primary tumor) displayed 90
227 differentially expressed genes between Matrigel 04 and Cultrex 87, whereas mT69A (KPC PDA
228 metastasis) presented with 13 (**Supplementary Figure 9B**). These results indicate that BME
229 does not substantially alter PDO gene expression profiles.

230 Previous work defined molecular subtypes of PDA. Patients with basal-like PDA exhibit
231 poor prognoses and increased therapeutic resistance compared to the classical subtype (*24*).
232 Changes to molecular subtype would have major implications on the predictive power of PDOs in
233 precision medicine approaches. To determine whether BME influenced hPDO subtype
234 classification, we delineated significant changes to enrichment of basal-like and classical

differentially expressed genes (see **Supplementary File** for gene list). Pairwise comparisons of subtype gene enrichment indicated no significant difference in basal-like or classical gene enrichment between Matrigel 04 and Matrigel 01, or between Cultrex 83 and Cultrex 87 (**Supplementary Figure 9E**). Notably, a number of comparisons that were enriched for one hallmark type were also enriched for the other (**Supplementary Figure 9E**). For instance, hM1F displayed upregulation of both basal-like as well as classical hallmark genes when cultured in Cultrex 83, Cultrex 87, or UltiMatrix **(Supplementary Figure 9E**)**.** Indeed, overall, there was a greater enrichment for the classical subtype signature, in concordance with previous work demonstrating that organoid models primarily exhibit RNA states reminiscent of the classical subtype (*16*). Analysis of individual genes implicated in the etiology of PDA revealed that BME did not significantly alter hPDO expression levels of *KRAS*, *TP53*, or *CDKN2A.* A slight but statistically significant increase in *SMAD4* expression was detected in hM1F cultured in Matrigel 01 compared to Matrigel 04 (**Figure 4B**). Similarly, we observed slight yet statistically significant increases in *ERBB3* in all three hPDOs cultured in Cultrex or UltiMatrix (**Supplementary Figure 9H**). Expression of *EGFR* was increased in hT1 cultured in Cultrex 87 relative to Matrigel 04 (**Supplementary Figure 9H**). However, we did not observe any significant changes in expression levels of *MYC*, *GATA6*, *MAP2K1*, *MAP2K2*, *SOX9*, *RB1*, *BRCA2*, and *ERBB2*, as well as genes related to drug resistance such as *HNF1A* and *ABCB1* (**Supplementary Figure 9H**). Overall, these data indicate that the potential influence of BME on organoid gene expression, cell state, and subsequent response to targeted therapies, must be carefully considered when developing protocols for organoid-guided therapy studies.

Discussion

The ability of PDOs to mirror patient genetics, transcriptomics, and drug response in retrospective studies prompted the onset of several clinical trials to test the benefit of using PDOs to inform treatment decisions. However, previous studies demonstrated the plasticity of PDOs in

261 response to varying culture conditions and potential impact on drug response (*16, 17*). With multi-
262 institutional clinical trials underway, the need to investigate factors that impact the robustness of
263 PDO genetics, transcriptomics, and drug testing is imperative. Basement membrane extracts are
264 central to most PDO efforts. Previous studies demonstrated variability in protein composition,
265 presence of xenogenic bioactive compounds, and scaffold stiffness between batches. Despite
266 this variability, commercially available BMEs remain critical and prevalent in organoid efforts.
267 Given the multi-year nature of PDO-related clinical trials, more than one lot of BME will be required
268 for the duration of these studies. In addition, limitations in availability due to supply chain issues
269 has necessitated that some efforts switch between alternate commercial sources. However, the
270 influence of BME source and lot on organoid response to drug treatment was unknown.

271 To investigate the extent to which BME impacts growth, drug response, and
272 transcriptomics, we compared various commercially available BMEs on previously established
273 mouse and human PDA organoids. We consistently observed a decrease in mouse and human
274 organoid growth when cultured in Cultrex or UltiMatrix compared to Matrigel. While this could
275 potentially arise from a lack of an adaptation period, multiple passages of mouse organoids in
276 Cultrex does not rescue their growth rate. Despite this growth deficit, we observed no substantial
277 shifts in drug response or gene expression as a function of BME source or lot. The generation
278 efficiency of PDA organoids in Matrigel is 75% (*8*). This study made use of previously established
279 organoids. Given the impact of BME source on PDO growth, it will be important to delineate the
280 effect of BME on isolation efficiency in future work. For established organoids, Matrigel, Cultrex,
281 or UltiMatrix BMEs are all viable options for pharmacotyping experiments. Altogether, this work
282 demonstrates that precision medicine approaches using organoids are robust, and that ongoing
283 clinical trials are unlikely to be affected by different lots or commercial sources of BME.

284

285 **Methods**

286 *Organoids and cell culture conditions*

287 Organoids used in this study were generated at Cold Spring Harbor Laboratory (*7, 8, 25*).
288 Human patient-derived and mouse organoids were cultured as described. In short, mouse
289 organoid media contained Advanced DMEM/F12, HEPES, Glutamax, Penicillin/Streptomycin,
290 EGF, FGF-10, Gastrin, A83-01, B27 supplement, *N*-acetylcysteine, nicotinamide, Noggin, and R-
291 spondin1. For human organoid culture, Wnt3a was also included in the media. Organoid
292 nomenclature is defined as: hT – human tumor obtained from resection; hF – human fine-needle
293 biopsy obtained by fine-needle aspiration or core biopsy; hM – human metastasis obtained from
294 direct resection of metastases following rapid autopsy or VATS resection; mT – murine tumor. All
295 organoid models were routinely tested for *Mycoplasma* at Salk Institute. Additional hPDO and
296 mouse organoid characteristics are available in **Table S1** and **Table S2**.
297
298 *Basement membrane extracts*
299 Both human and mouse organoids were maintained in Corning Matrigel Lot #1062004
300 during the growth and expansion phase. For pharmacotyping comparisons, organoids were plated
301 in either Corning Matrigel (Growth Factor Reduced, Phenol Red Free) Lot #1062004 (Matrigel
302 04), Corning Matrigel (Growth Factor Reduced, Phenol Red Free) Lot #0287001 (Matrigel 01),
303 RnD Cultrex Reduced Growth Factor BME Lot #1564183 (Cultrex 83), RnD Cultrex Reduced
304 Growth Factor BME Lot #1586187 (Cultrex 87), or Cultrex UltiMatrix Reduced Growth Factor BME
305 Lot #1637796 (UltiMatrix 96).
306
307 *Pharmacotyping of organoids*
308 Organoids were dissociated into single cells using a diluted solution of TrypLE Express
309 (Thermo Fisher). Equal numbers of single cells (1,500 viable cells per well) were plated in a 20
310 uL suspension of 10% BME in ultra-low attachment 384 well plates (Corning). Twenty-four hours
311 after plating, reformation of organoids was visually verified and therapeutic compounds were
312 applied using a digital dispenser (Tecan). Chemotherapies were tested in triplicate 10-point dose-

313 response curves. Gemcitabine, paclitaxel, SN-38 (active metabolite of irinotecan), and trametinib
314 ranged from 0.5nM – 5μM; oxaliplatin and 5-fluorouracil ranged from 50nM – 100μM. Compounds
315 were dissolved in DMSO, and all treatments were normalized to 0.5% DMSO content. Mouse
316 organoids underwent treatment for 3 days, while human organoids underwent treatment for 5
317 days. After treatment, cell viability was assessed using Cell Titer Glo (Promega) per
318 manufacturer's instructions on a Tecan Spark Cyto plate reader. A four-parameter log-logistic
319 function with upper limit equal to the mean of the lowest dose values was fit to the data (viability
320 vs. dose) with Graphpad Prism 9. The half maximal inhibitory concentration (IC50) values, area
321 under the curve (AUC), and standard deviation of the residuals (Sy.x) for each dose-response
322 curve were calculated using Graphpad Prism 9. Each pharmacotyping experiment was carried
323 out at least two times.
324
325 *RNA isolation*
326 For RNA-seq comparisons, organoids were maintained in Corning Matrigel Lot #1062004
327 (Matrigel 04) and then plated in either Corning Matrigel (Growth Factor Reduced, Phenol Red
328 Free) Lot #1062004 (Matrigel 04), Corning Matrigel (Growth Factor Reduced, Phenol Red Free)
329 Lot #0287001 (Matrigel 01), RnD Cultrex Reduced Growth Factor BME Lot #1564183 (Cultrex
330 83), RnD Cultrex Reduced Growth Factor BME Lot #1586187 (Cultrex 87), or Cultrex UltiMatrix
331 Reduced Growth Factor BME Lot #1637796 (Ultimatrix 96). Each BME condition was plated in
332 triplicate, and organoids were grown for 3 days before harvesting in TRIzol (Life Technologies)
333 and snap frozen. RNA was isolated using the RNeasy Mini Kit (Qiagen). RNA quality control was
334 performed for all samples using a Qubit Fluorometer (Life Technologies) and TapeStation (RIN
335 greater than 8.5) (Agilent) before RNA-seq analyses.
336
337 *RNA-seq analyses*

338 Library construction was conducted using the Truseq RNA library prep kit (Illumina) with
339 500ng RNA input. Raw reads were trimmed with Trim Galore v0.4.4_dev
340 (https://www.bioinformatics.babraham.ac.uk/projects/trim_galore/) and quality-checked with
341 FastQC v0.11.8 (http://www.bioinformatics.babraham.ac.uk/projects/fastqc). Trimmed reads
342 were then aligned to the hg38 human reference genome with STAR aligner v2.5.3a (*26*), and
343 converted to gene counts with HOMER's analyzeRepeats.pl script (*27*).
344
345 *Differential gene expression analysis*
346 Gene counts where normalized and queried for differential expression using DESeq2
347 v1.30.0 (*28*). For each pairwise comparison, genes with fewer than 10 total raw counts across all
348 samples were discarded prior to normalization, and genes with an absolute log2foldchange > 1
349 and an FDR-corrected p-value ≤ 0.05 were pulled as significant.
350
351 *Statistics*
352 A four-parameter log-logistic function with upper limit equal to the mean of the lowest dose
353 values was fit to the dose-response data (viability vs. dose) with Graphpad Prism 9. The half
354 maximal inhibitory concentration (IC50) values, area under the curve (AUC), and standard
355 deviation of the residuals (Sy.x) for each dose-response curve were calculated using Graphpad
356 Prism 9. Each pharmacotyping experiment was carried out for n = 2-4 experimental replicates.
357 Differences among means were analyzed using 1-way ANOVA with Dunnett's multiple
358 comparisons test. Outliers were determined using Grubbs' test α = 0.05.
359 To compare estimated dose-response curve parameters across different BMEs within an
360 experimental replicate, t-tests were conducted on the IC50 and Hill slope to test the null
361 hypothesis of zero difference in the parameters among BMEs using R 4.0.3 and package drc (*22,*
362 *29*). The Bonferroni method was used to adjust for multiple comparisons, and a comparison
363 between a pair of BMEs was considered significant if the *P* value was below 0.05 divided by the

364 total number of pairwise comparisons. Consequently, pairwise t-tests were considered significant
365 if $P < 0.00027778$ (hPDO) or $P < 0.00041667$ (mouse organoids).
366 To assess the model fitting and compare the log-logistic models with other alternatives,
367 including Weibull models, a sensitivity analysis was conducted. The Akaike Information Criterion
368 (AIC) was used for the comparison. The four-parameter log-logistic (LL4) model consistently
369 yielded smaller AIC values, suggesting this model as the most appropriate model-fitting strategy.
370 Analyses presented from the aforementioned t-tests on IC50 and Hill slope were conducted first
371 on data fitted with the LL4 model, then on data fitted with Weibull models when appropriate.
372
373 *Author contributions*
374 JL, SO, and KP maintained organoid cultures, acquired materials, and designed and
375 conducted the experiments. JL and XL acquired and analyzed the data. KL performed statistical
376 analysis on RNA-seq data. JZ directed and provided statistical analysis for dose-response curve
377 comparisons. JL, XL, JZ, and DE wrote the manuscript. DE conceived the project and directed
378 the experiments.
379
380 *Acknowledgements*
381 The authors are supported by National Institutes of Health, National Cancer Institute
382 R00CA024725 (Engle), P30DK120515 (Engle), T32CA009370 (Lumibao); the Pancreatic Cancer
383 Action Network 19-20-ENGL (Engle), American Association for Cancer Research and the
384 Lustgarten Foundation 21-20-67-ENGL (Engle), the University of California Tobacco-Related
385 Disease Research Program T31KT1898 (Engle), and Padres Pedal the Cause/C3 #PTC2020
386 (Engle). We are grateful to the Rose Hills Foundation, Mission Cure Capital, LLC, the Mark
387 Foundation for Cancer Research, and the Emerald Foundation, Inc. for supporting Dr. Engle.
388 Additionally, this work was supported by the Razavi Newman Integrative Genomics and
389 Bioinformatics Core Facility of the Salk Institute with funding from NIH-NCI CCSG: P30 014195,

and the Helmsley Trust; the NGS Core Facility of the Salk Institute with funding from NIH-NCI CCSG: P30 014195, the Chapman Foundation and the Helmsley Charitable Trust; and the Stem Cell Core Facility of the Salk Institute with funding from the Helmsley Charitable Trust.

Figure legends

Figure 1. Basement membrane extract impacts growth of mouse and human organoids but does not significantly shift dose-response curves. (**A**) Growth of human patient-derived organoids hF24 and hM1F cultured in Matrigel 04, Matrigel 01, Cultrex 83, Cultrex 87, or UltiMatrix 96 for 5 days as determined by levels of intracellular ATP (Cell Titer Glo - CTG). Data represent mean ± SD. Statistical significance was determined by 1-way ANOVA. ****$P \leq 0.0001$. (**B**) Growth of mouse organoids mT69A and mT69B cultured in Matrigel 04, Matrigel 01, Cultrex 83, Cultrex 87, or UltiMatrix 96 for 3 days as determined by levels of intracellular ATP (CTG). Data represent mean ± SD. Statistical significance was determined by 1-way ANOVA. ****$P \leq 0.0001$. (**C**) Dose-response curves for hF24 treated with gemcitabine, paclitaxel, SN-38, oxaliplatin, 5-FU, and trametinib during culture in Matrigel 04, Matrigel 01, Cultrex 83, Cultrex 87, or UltiMatrix 96. Data represent mean ± SD of triplicate values fitted with a four-parameter log-logistic function. (**D**) Dose-response curves for mT69B treated with gemcitabine, paclitaxel, SN-38, oxaliplatin, 5-FU, and trametinib during culture in Matrigel 04, Matrigel 01, Cultrex 83, Cultrex 87, or UltiMatrix 96. Data represent mean ± SD of triplicate values fitted with a four-parameter log-logistic function.

Figure 2. Basement membrane extracts exert minimal effects on drug IC50 and dose-response AUC. (**A-B**) *P* value heatmaps from pairwise comparisons of IC50 between BMEs for hF24 and hM1F. Each square represents pairwise t-tests. After Bonferroni adjustment, t-tests were considered significant if $P < 0.00027778$. Statistically significant comparisons are denoted by an asterisk and orange border. (**C-D**) Gemcitabine, paclitaxel, SN-38, oxaliplatin, 5-FU, and trametinib IC50 values (M) for hF24 and hM1F across different BMEs. Data represent mean ± SD

416 of 3 experimental replicates. (**E-F**) Gemcitabine, paclitaxel, SN-38, oxaliplatin, 5-FU, and
417 trametinib AUC values for hF24 and hM1F across the different BMEs. Data represent mean ± SD
418 of 3 experimental replicates. Statistical significance was determined by 1-way ANOVA. *$P \leq 0.05$,
419 ***$P \leq 0.001$ vs. Matrigel 04.
420
421 **Figure 3. Dose-response curve goodness of fit is not significantly altered by basement**
422 **membrane extract.** (**A-B**) Standard deviation of the residuals (Sy.x) for hF24 and hM1F treated
423 with gemcitabine, paclitaxel, SN-38, oxaliplatin, 5-FU, and trametinib across the different BMEs.
424 Data represent mean ± SD of 3 experimental replicates. (**C-D**) Sy.x for mT69A and mT69B treated
425 with gemcitabine, paclitaxel, SN-38, oxaliplatin, 5-fluorourical (5-FU), and trametinib across the
426 different BMEs. Data represent mean ± SD of 4 experimental replicates. Outliers were determined
427 using Grubbs' test α = 0.05.
428
429 **FIgure 4. Human patient-derived organoid gene expression profiles are consistent across**
430 **basement membrane extract types.** (**A**) Expression heatmap of Z-scores of normalized counts
431 of classical or basal-like hallmark genes in hF24, hM1F, and hT1 when cultured in different BMEs.
432 (B) Normalized counts for hallmark PDA genes *KRAS, TP53, SMAD4,* and *CDKN2A*. Data
433 represent mean ± SD of 3 technical replicates. Statistical significance was determined by 1-way
434 ANOVA. **$P \leq 0.01$ vs. Matrigel 04.
435
436 **Supplementary Figure 1. Experimental outline.** Three biological replicates of human patient-
437 derived organoids and mouse organoids were selected based on primary sample type and
438 disease stage. Each organoid line was expanded to sufficient quantities for experimentation in
439 Matrigel 04. Organoids were then single-cell dissociated and either plated in triplicate in 6-well
440 plates for RNA isolation and subsequent RNA-seq, or plated for pharmacotyping in five 384-well
441 plates in Matrigel 04, Matrigel 01, Cultrex 83, Cultrex 87, or UltiMatrix 96. Organoids were allowed

442 to recover overnight. Next, organoids were treated with drugs and incubated for 5 days (human
443 organoids) or 3 days (mouse organoids), followed by Cell Titer Glo to assess organoid viability.
444
445 **Supplementary Figure 2. Proliferation of human and mouse organoids is not significantly**
446 **altered by basement membrane extract.** (**A**) Data for n = 3 experimental replicates of hF24
447 proliferation in Matrigel 04, Matrigel 01, Cultrex 83, Cultrex 87, or UltiMatrix 96. Data represent
448 mean ± SD. ****P* ≤ 0.01, *****P* ≤ 0.0001 vs. Matrigel 04. (**B**) Data for n = 3 experimental replicates
449 of hM1F proliferation in Matrigel 04, Matrigel 01, Cultrex 83, Cultrex 87, or UltiMatrix 96. Data
450 represent mean ± SD. ****P* ≤ 0.01, *****P* ≤ 0.0001 vs. Matrigel 04. (**C**) Data for n = 2 experimental
451 replicates of hT1 proliferation in Matrigel 04, Matrigel 01, Cultrex 83, Cultrex 87, or UltiMatrix 96.
452 Data represent mean ± SD. *****P* ≤ 0.0001 vs. Matrigel 04. (**D**) Data for n = 4 experimental
453 replicates of mT69A proliferation in Matrigel 04, Matrigel 01, Cultrex 83, Cultrex 87, or UltiMatrix
454 96. Data represent mean ± SD. **P* ≤ 0.05, ****P* ≤ 0.01, *****P* ≤ 0.0001 vs. Matrigel 04. (**E**) Data for
455 n = 4 experimental replicates of mT69B proliferation in Matrigel 04, Matrigel 01, Cultrex 83, Cultrex
456 87, or UltiMatrix 96. Data represent mean ± SD. ****P* ≤ 0.01, *****P* ≤ 0.0001 vs. Matrigel 04.
457
458 **Supplementary Figure 3. Dose response curves are consistent regardless of basement**
459 **membrane extract used.** (**A**) Data for n = 3 experimental replicates of hF24 response to
460 gemcitabine, paclitaxel, SN-38, oxaliplatin, 5-FU, and trametinib while cultured in Matrigel 04,
461 Matrigel 01, Cultrex 83, Cultrex 87, or UltiMatrix 96. Data represent mean ± SD. (**B**) Data for n =
462 3 experimental replicates of hM1F response to gemcitabine, paclitaxel, SN-38, oxaliplatin, 5-FU,
463 and trametinib while cultured in Matrigel 04, Matrigel 01, Cultrex 83, Cultrex 87, or UltiMatrix 96.
464 Data represent mean ± SD. (**C**) Data for n = 2 experimental replicates of hT1 response to
465 gemcitabine, paclitaxel, SN-38, oxaliplatin, 5-FU, and trametinib while cultured in Matrigel 04,
466 Matrigel 01, Cultrex 83, Cultrex 87, or UltiMatrix 96. Data represent mean ± SD. (**D**) Data for n =
467 4 experimental replicates of mT69A response to gemcitabine, paclitaxel, SN-38, oxaliplatin, 5-FU,

468 and trametinib while cultured in Matrigel 04, Matrigel 01, Cultrex 83, Cultrex 87, or UltiMatrix 96.
469 Data represent mean ± SD. (**E**) Data for n = 4 experimental replicates of mT69B response to
470 gemcitabine, paclitaxel, SN-38, oxaliplatin, 5-FU, and trametinib while cultured in Matrigel 04,
471 Matrigel 01, Cultrex 83, Cultrex 87, or UltiMatrix 96. Data represent mean ± SD.
472
473 **Supplementary Figure 4. Statistically significant differences in IC50 within experimental**
474 **replicates occur on a per-drug and per-organoid basis.** (**A-C**) Heatmaps of *P* values from
475 pairwise comparisons of IC50 between BMEs for each experimental repeat of hF24 (**A**), hM1F
476 (**B**), or hT1 (**C**). Each square represents significance of pairwise t-tests. After Bonferroni
477 adjustment, t-tests were considered significant if $P < 0.00027778$. Statistically significant
478 comparisons are denoted by an asterisk and orange border. (**D-E**) Heatmaps of *P* values from
479 pairwise comparisons of IC50 between BMEs for each experimental repeat of mT69A (**D**) or
480 mT69B (**E**). Each square represents significance of pairwise t-tests. After Bonferroni adjustment,
481 t-tests were considered significant if $P < 0.00041667$. Statistically significant comparisons are
482 denoted by an asterisk and orange border.
483
484 **Supplementary Figure 5. Dose response curve Hill slopes remain consistent across**
485 **basement membrane extract culture conditions.** (**A-C**) Heatmaps of *P* values from pairwise
486 comparisons of Hill slope between BMEs for each experimental repeat of hF24 (**A**), hM1F (**B**), or
487 hT1 (**C**). Each square represents significance of pairwise t-tests. After Bonferroni adjustment, t-
488 tests were considered significant if $P < 0.00027778$. Statistically significant comparisons are
489 denoted by an asterisk and orange border. (**D-E**) Heatmaps of *P* values from pairwise
490 comparisons of Hill slope between BMEs for each experimental repeat of mT69A (**D**) or mT69B
491 (**E**). Each square represents significance of pairwise t-tests. After Bonferroni adjustment, t-tests
492 were considered significant if $P < 0.00041667$. Statistically significant comparisons are denoted
493 by an asterisk and orange border.

494

495 **Supplementary Figure 6. IC50 values remain consistent across basement membrane**
496 **extract culture conditions.** (**A**) IC50 values (M) for hT1 treated with gemcitabine, paclitaxel, SN-
497 38, oxaliplatin, 5-FU, and trametinib during culture in Matrigel 04, Matrigel 01, Cultrex 83, Cultrex
498 87, or UltiMatrix 96. Data represent mean ± SD of 2 experimental replicates. (**B**) IC50 values (M)
499 for mT69A treated with gemcitabine, paclitaxel, SN-38, oxaliplatin, 5-FU, and trametinib during
500 culture in Matrigel 04, Matrigel 01, Cultrex 83, Cultrex 87, or UltiMatrix 96. Data represent mean
501 ± SD of 4 experimental replicates. (**C**) IC50 values (M) for mT69B treated with gemcitabine,
502 paclitaxel, SN-38, oxaliplatin, 5-FU, and trametinib during culture in Matrigel 04, Matrigel 01,
503 Cultrex 83, Cultrex 87, or UltiMatrix 96. Data represent mean ± SD of 4 experimental replicates.
504 Outliers were determined using Grubbs' test α = 0.05.

505

506 **Supplementary Figure 7. AUC values are consistent across basement membrane extract**
507 **culture conditions.** (**A**) AUC values for hT1 treated with gemcitabine, paclitaxel, SN-38,
508 oxaliplatin, 5-FU, and trametinib during culture in Matrigel 04, Matrigel 01, Cultrex 83, Cultrex 87,
509 or UltiMatrix 96. Data represent mean ± SD of 2 experimental replicates. (**B**) AUC values for
510 mT69A treated with gemcitabine, paclitaxel, SN-38, oxaliplatin, 5-FU, and trametinib during
511 culture in Matrigel 04, Matrigel 01, Cultrex 83, Cultrex 87, or UltiMatrix 96. Data represent mean
512 ± SD of 4 experimental replicates. Statistical significance was determined by 1-way ANOVA. *P
513 ≤ 0.05 vs. Matrigel 04. (**C**) AUC values for mT69B treated with gemcitabine, paclitaxel, SN-38,
514 oxaliplatin, 5-FU, and trametinib during culture in Matrigel 04, Matrigel 01, Cultrex 83, Cultrex 87,
515 or UltiMatrix 96. Data represent mean ± SD of 4 experimental replicates.

516

517 **Supplementary Figure 8. Standard deviation of the residuals does not statistically change**
518 **as a function of basement membrane extract used.** Standard deviation of the residuals (Sy.x)
519 for hT1 treated with gemcitabine, paclitaxel, SN-38, oxaliplatin, 5-fluorourical (5-FU), and

520 trametinib during culture in Matrigel 04, Matrigel 01, Cultrex 83, Cultrex 87, or UltiMatrix 96. Data
521 represent mean ± SD of 2 experimental replicates. Outliers were determined using Grubbs' test
522 α = 0.05.
523
524 **Supplementary Figure 9. Global gene expression profiles are consistent across basement**
525 **membrane extract conditions for both mouse and human organoids.** (**A**) Differential gene
526 expression among human patient-derived organoids cultured in Matrigel 04 (MG004), Matrigel 01
527 (MG001), Cultrex 83 (Cultrex 183), Cultrex 87 (Cultrex 187), or UltiMatrix 96 (Ultimatrix). Numbers
528 represent total number of genes with an adjusted *P* value of differential expression ≤ 0.05 and an
529 absolute log2(foldchange) > 1 for all pairwise comparisons of basement membrane extracts within
530 individual organoid lines and within species. (**B**) Differential gene expression among mouse
531 organoids cultured in Matrigel 04 (MG004), Matrigel 01 (MG001), Cultrex 83 (Cultrex 183), Cultrex
532 87 (Cultrex 187), or UltiMatrix 96 (Ultimatrix). Numbers represent total number of genes with an
533 adjusted *P* value of differential expression ≤ 0.05 and an absolute log2(foldchange) > 1 for all
534 pairwise comparisons of basement membrane extracts within individual organoid lines and within
535 species. (**C**) Principal component analysis of human patient-derived organoid gene expression
536 within species and individual organoid lines. (**D**) Principal component analysis of mouse organoid
537 gene expression within species and individual organoid lines. (**E**) Heatmaps of basal-like or
538 classical hallmark gene enrichment between basement membrane extract comparisons for all
539 human patient-derived organoid lines (top row) and individual lines. Each square represents
540 significance of enrichment in the differentially expressed genes between two basement
541 membrane extracts. The differentially expressed genes in the BME listed on the y-axis are queried
542 for enrichment. Squares are labeled with *P* value. Black squares = ns. (**F**) Expression heatmap
543 of all genes in human patient-derived organoids cultured in different BMEs. Z-scores of
544 normalized counts. (**G**) Expression heatmap of all genes in mouse organoids cultured in different
545 basement membrane extracts. Z-scores of normalized counts. (**H**) Normalized counts for select

546 genes of interest in hF24, hM1F, and hT1 cultured in different BMEs. Data represent mean ± SD
547 of 3 technical replicates. *$P \leq 0.05$, **$P \leq 0.01$ vs. Matrigel 04.
548
549
550
551
552
553
554
555
556
557
558
559
560
561
562
563
564
565
566
567
568
569
570
571

572 **References**

573 1. American Cancer Society. Cancer Facts & Figures 2023. (2023).

574 2. R. Abbassi, H. Algül, Palliative chemotherapy in pancreatic cancer-treatment sequences.
575 *Transl Gastroenterol Hepatol* **4**, 56 (2019).

576 3. J. Kleeff *et al.*, Pancreatic cancer. *Nat Rev Dis Primers* **2**, 16022 (2016).

577 4. D. D. Von Hoff *et al.*, Increased survival in pancreatic cancer with nab-paclitaxel plus
578 gemcitabine. *N Engl J Med* **369**, 1691-1703 (2013).

579 5. T. Conroy *et al.*, FOLFIRINOX versus gemcitabine for metastatic pancreatic cancer. *N*
580 *Engl J Med* **364**, 1817-1825 (2011).

581 6. T. T. Seppälä *et al.*, Patient-derived Organoid Pharmacotyping is a Clinically Tractable
582 Strategy for Precision Medicine in Pancreatic Cancer. *Ann Surg* **272**, 427-435 (2020).

583 7. S. F. Boj *et al.*, Organoid models of human and mouse ductal pancreatic cancer. *Cell* **160**,
584 324-338 (2015).

585 8. H. Tiriac *et al.*, Organoid Profiling Identifies Common Responders to Chemotherapy in
586 Pancreatic Cancer. *Cancer Discov* **8**, 1112-1129 (2018).

587 9. L. Huang *et al.*, Ductal pancreatic cancer modeling and drug screening using human
588 pluripotent stem cell- and patient-derived tumor organoids. *Nat Med* **21**, 1364-1371
589 (2015).

590 10. L. Huang *et al.*, PDX-derived organoids model in vivo drug response and secrete
591 biomarkers. *JCI Insight* **5**, (2020).

592 11. L. Huang *et al.*, Commitment and oncogene-induced plasticity of human stem cell-derived
593 pancreatic acinar and ductal organoids. *Cell Stem Cell* **28**, 1090-1104.e1096 (2021).

594 12. E. Driehuis, K. Kretzschmar, H. Clevers, Establishment of patient-derived cancer
595 organoids for drug-screening applications. *Nat Protoc* **15**, 3380-3409 (2020).

596 13. E. Driehuis *et al.*, Pancreatic cancer organoids recapitulate disease and allow
597 personalized drug screening. *Proceedings of the National Academy of Sciences of the*
598 *United States of America* **116**, 26580-26590 (2019).
599 14. S. Hou *et al.*, Advanced Development of Primary Pancreatic Organoid Tumor Models for
600 High-Throughput Phenotypic Drug Screening. *SLAS Discov* **23**, 574-584 (2018).
601 15. T. T. Seppälä *et al.*, Precision Medicine in Pancreatic Cancer: Patient-Derived Organoid
602 Pharmacotyping Is a Predictive Biomarker of Clinical Treatment Response. *Clinical cancer*
603 *research : an official journal of the American Association for Cancer Research* **28**, 3296-
604 3307 (2022).
605 16. S. Raghavan *et al.*, Microenvironment drives cell state, plasticity, and drug response in
606 pancreatic cancer. *Cell* **184**, 6119-6137.e6126 (2021).
607 17. T. L. Hogenson *et al.*, Culture media composition influences patient-derived organoid
608 ability to predict therapeutic responses in gastrointestinal cancers. *JCI Insight* **7**, (2022).
609 18. N. Broguiere *et al.*, Growth of Epithelial Organoids in a Defined Hydrogel. *Adv Mater* **30**,
610 e1801621 (2018).
611 19. E. A. Aisenbrey, W. L. Murphy, Synthetic alternatives to Matrigel. *Nat Rev Mater* **5**, 539-
612 551 (2020).
613 20. S. Randriamanantsoa *et al.*, Spatiotemporal dynamics of self-organized branching in
614 pancreas-derived organoids. *Nat Commun* **13**, 5219 (2022).
615 21. S. Khan, H. Tiriac, Synthetic scaffold for pancreatic organoids. *Nat Mater* **21**, 9-11 (2022).
616 22. C. Ritz, J. C. Streibig, Bioassay analysis using R. *Journal of Statistical Software* **12**, 1-22
617 (2005).
618 23. N. E. Webb, D. C. Montefiori, B. Lee, Dose-response curve slope helps predict therapeutic
619 potency and breadth of HIV broadly neutralizing antibodies. *Nat Commun* **6**, 8443 (2015).
620 24. R. A. Moffitt *et al.*, Virtual microdissection identifies distinct tumor- and stroma-specific
621 subtypes of pancreatic ductal adenocarcinoma. *Nat Genet* **47**, 1168-1178 (2015).

622 25. J. S. Roe *et al.*, Enhancer Reprogramming Promotes Pancreatic Cancer Metastasis. *Cell*
623 **170**, 875-888.e820 (2017).
624 26. A. Dobin *et al.*, STAR: ultrafast universal RNA-seq aligner. *Bioinformatics* **29**, 15-21
625 (2013).
626 27. S. Heinz *et al.*, Simple combinations of lineage-determining transcription factors prime cis-
627 regulatory elements required for macrophage and B cell identities. *Mol Cell* **38**, 576-589
628 (2010).
629 28. M. I. Love, W. Huber, S. Anders, Moderated estimation of fold change and dispersion for
630 RNA-seq data with DESeq2. *Genome Biol* **15**, 550 (2014).
631 29. M. P. M., B. A., The combination of estimates from similar experiments, allowing for inter-
632 experiment variation. *Journal of the American Statistical Association* **62**, 241-250 (1967).
633

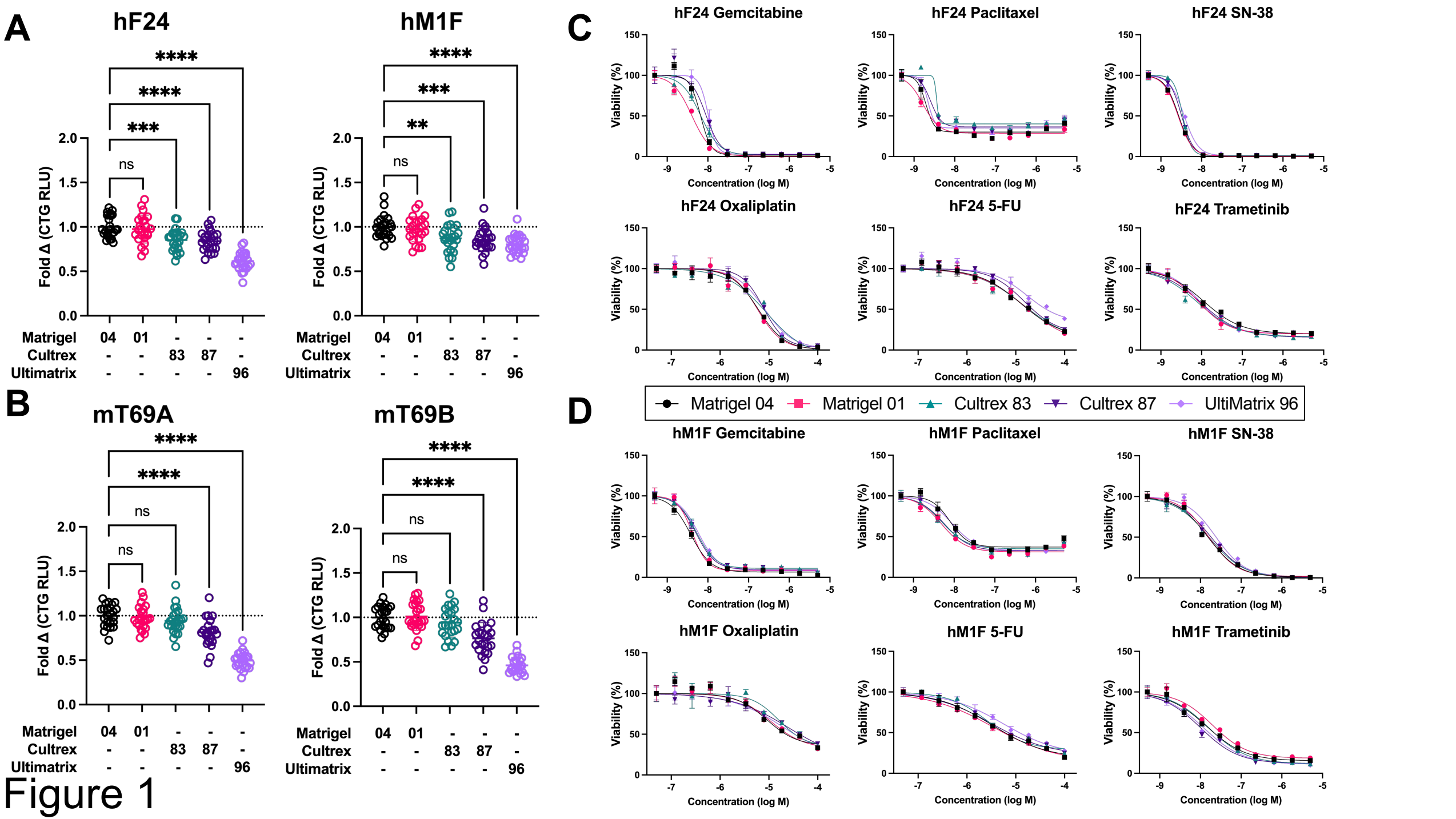
A
hF24
hM1F
B
mT69A
mT69B
Fold Δ (CTG RLU)
Matrigel 04 01 - - -
Cultrex - - 83 87 -
Ultimatrix - - - - 96
ns
**
***
****
C
hF24 Gemcitabine
hF24 Paclitaxel
hF24 SN-38
hF24 Oxaliplatin
hF24 5-FU
hF24 Trametinib
D
hM1F Gemcitabine
hM1F Paclitaxel
hM1F SN-38
hM1F Oxaliplatin
hM1F 5-FU
hM1F Trametinib
Viability (%)
Concentration (log M)
Matrigel 04
Matrigel 01
Cultrex 83
Cultrex 87
UltiMatrix 96

Figure 1

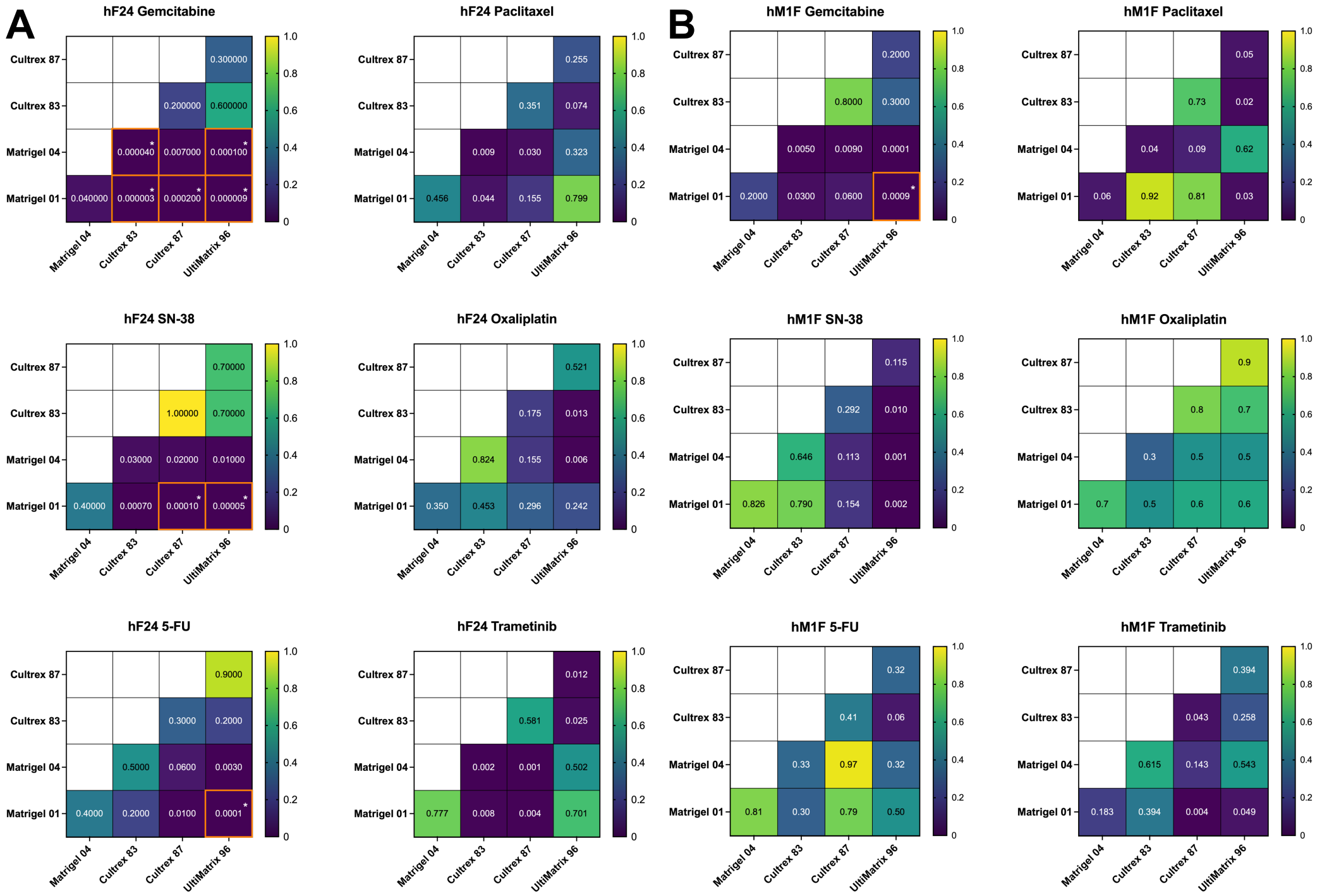
A
B
hF24 Gemcitabine
Cultrex 87 0.300000
Cultrex 83 0.200000 0.600000
Matrigel 04 0.000040* 0.007000 0.000100*
Matrigel 01 0.040000 0.000003* 0.000200* 0.000009*
hF24 Paclitaxel
Cultrex 87 0.255
Cultrex 83 0.351 0.074
Matrigel 04 0.009 0.030 0.323
Matrigel 01 0.456 0.044 0.155 0.799
hM1F Gemcitabine
Cultrex 87 0.2000
Cultrex 83 0.8000 0.3000
Matrigel 04 0.0050 0.0090 0.0001
Matrigel 01 0.2000 0.0300 0.0600 0.0009*
hM1F Paclitaxel
Cultrex 87 0.05
Cultrex 83 0.73 0.02
Matrigel 04 0.04 0.09 0.62
Matrigel 01 0.06 0.92 0.81 0.03
hF24 SN-38
Cultrex 87 0.70000
Cultrex 83 1.00000 0.70000
Matrigel 04 0.03000 0.02000 0.01000
Matrigel 01 0.40000 0.00070 0.00010* 0.00005*
hF24 Oxaliplatin
Cultrex 87 0.521
Cultrex 83 0.175 0.013
Matrigel 04 0.824 0.155 0.006
Matrigel 01 0.350 0.453 0.296 0.242
hM1F SN-38
Cultrex 87 0.115
Cultrex 83 0.292 0.010
Matrigel 04 0.646 0.113 0.001
Matrigel 01 0.826 0.790 0.154 0.002
hM1F Oxaliplatin
Cultrex 87 0.9
Cultrex 83 0.8 0.7
Matrigel 04 0.3 0.5 0.5
Matrigel 01 0.7 0.5 0.6 0.6
hF24 5-FU
Cultrex 87 0.9000
Cultrex 83 0.3000 0.2000
Matrigel 04 0.5000 0.0600 0.0030
Matrigel 01 0.4000 0.2000 0.0100 0.0001*
hF24 Trametinib
Cultrex 87 0.012
Cultrex 83 0.581 0.025
Matrigel 04 0.002 0.001 0.502
Matrigel 01 0.777 0.008 0.004 0.701
hM1F 5-FU
Cultrex 87 0.32
Cultrex 83 0.41 0.06
Matrigel 04 0.33 0.97 0.32
Matrigel 01 0.81 0.30 0.79 0.50
hM1F Trametinib
Cultrex 87 0.394
Cultrex 83 0.043 0.258
Matrigel 04 0.615 0.143 0.543
Matrigel 01 0.183 0.394 0.004 0.049
Matrigel 04
Cultrex 83
Cultrex 87
UltiMatrix 96
1.0
0.8
0.6
0.4
0.2
0

Figure 2A-B

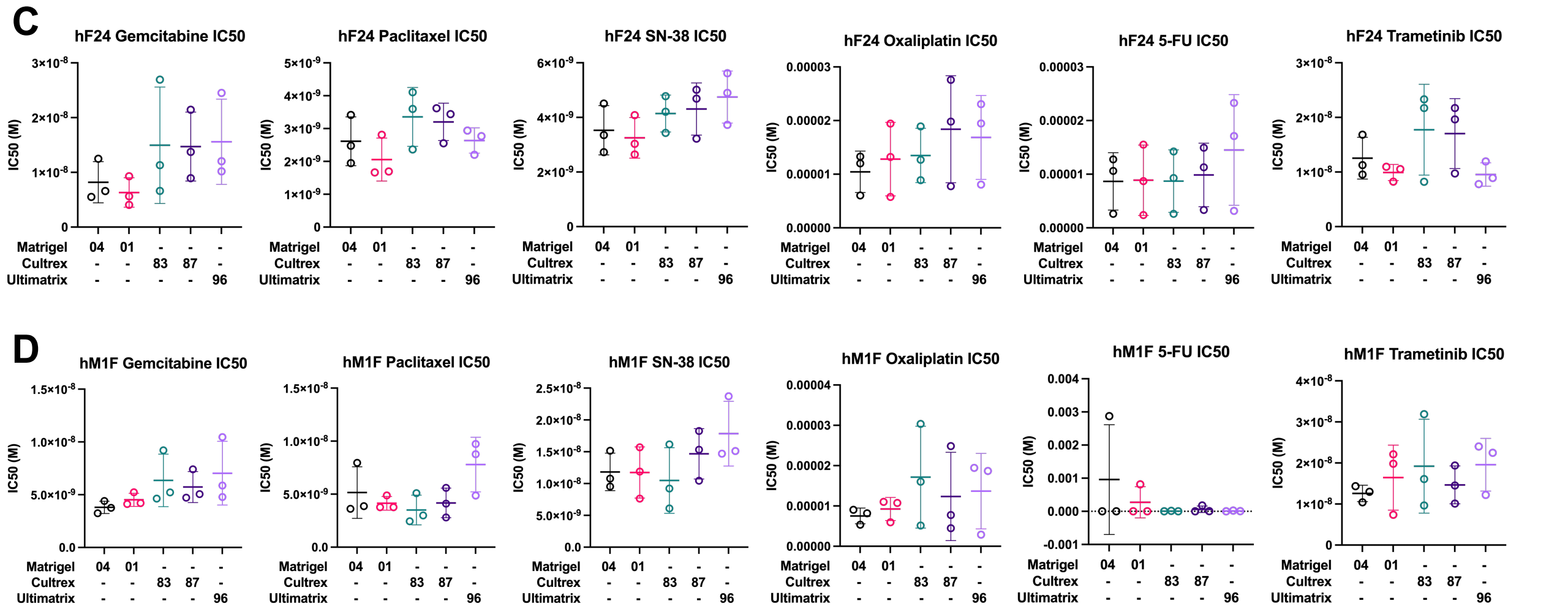
C
hF24 Gemcitabine IC50
hF24 Paclitaxel IC50
hF24 SN-38 IC50
hF24 Oxaliplatin IC50
hF24 5-FU IC50
hF24 Trametinib IC50
D
hM1F Gemcitabine IC50
hM1F Paclitaxel IC50
hM1F SN-38 IC50
hM1F Oxaliplatin IC50
hM1F 5-FU IC50
hM1F Trametinib IC50
IC50 (M)
Matrigel 04 01 - - -
Cultrex - - 83 87 -
Ultimatrix - - - - 96

Figure 2C-D

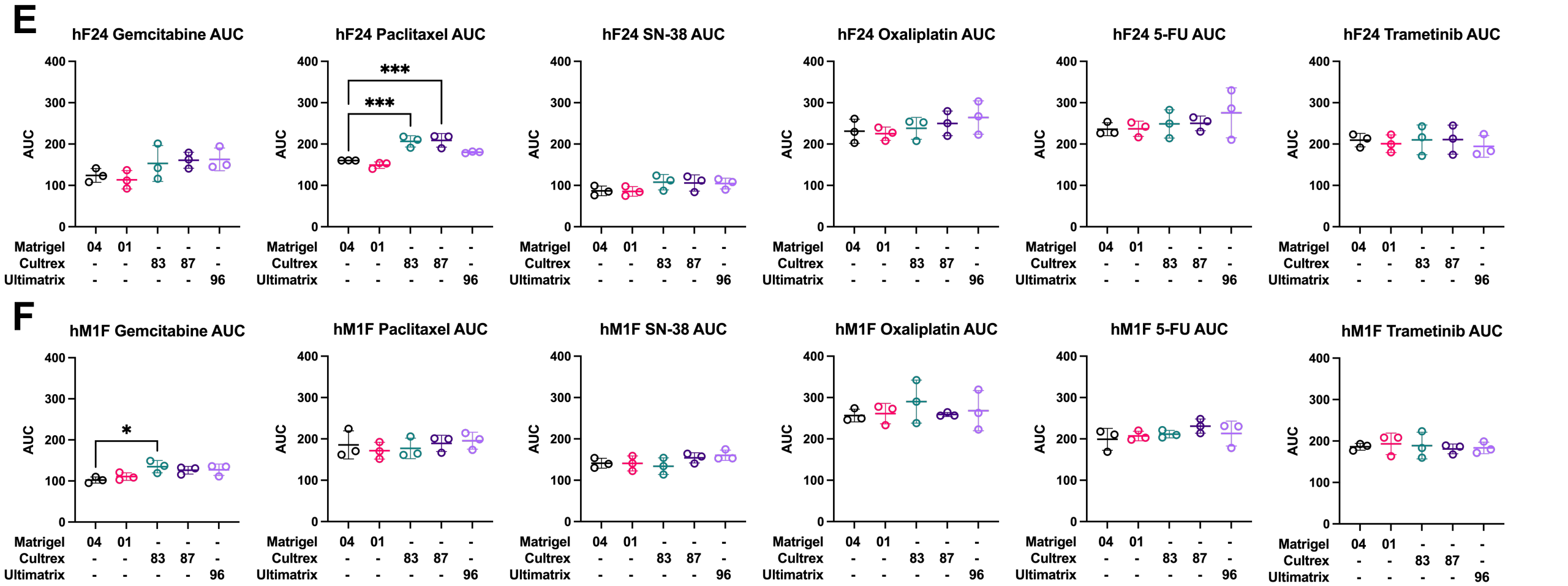
E
hF24 Gemcitabine AUC
hF24 Paclitaxel AUC
hF24 SN-38 AUC
hF24 Oxaliplatin AUC
hF24 5-FU AUC
hF24 Trametinib AUC
F
hM1F Gemcitabine AUC
hM1F Paclitaxel AUC
hM1F SN-38 AUC
hM1F Oxaliplatin AUC
hM1F 5-FU AUC
hM1F Trametinib AUC
AUC
0
100
200
300
400
***
*
Matrigel 04 01 - - -
Cultrex - - 83 87 -
Ultimatrix - - - - 96

Figure 2E-F

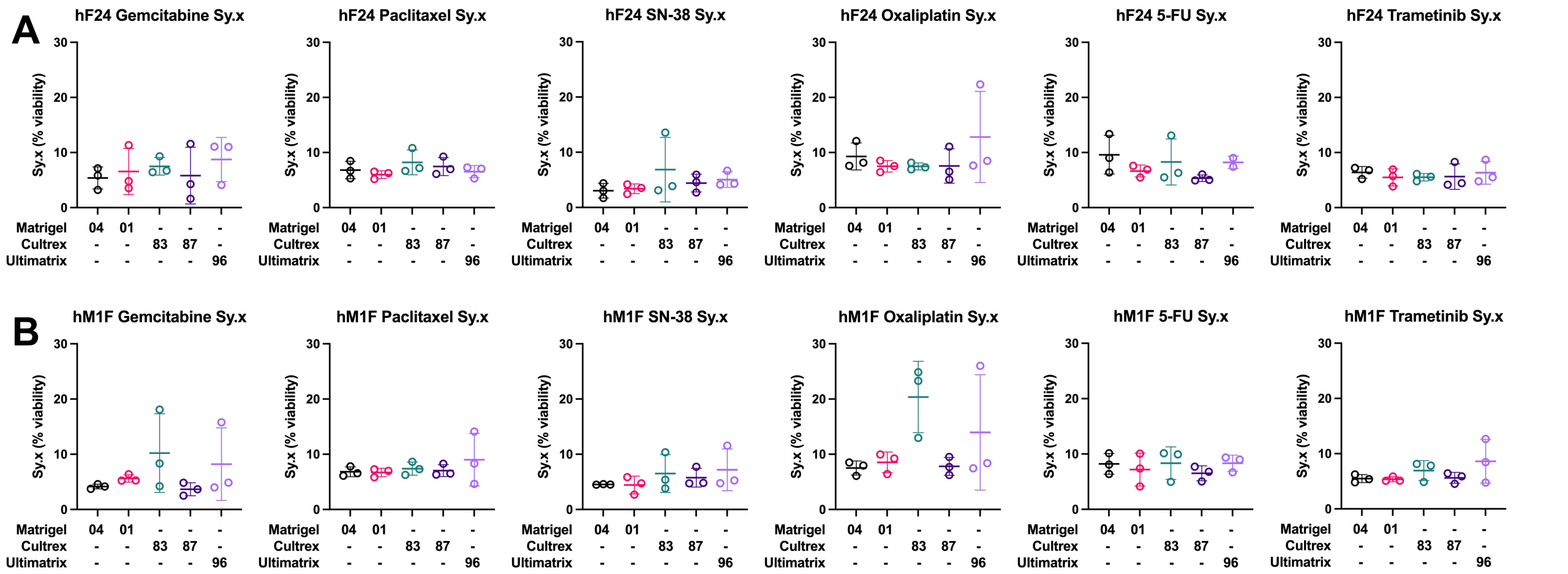
A
hF24 Gemcitabine Sy.x
hF24 Paclitaxel Sy.x
hF24 SN-38 Sy.x
hF24 Oxaliplatin Sy.x
hF24 5-FU Sy.x
hF24 Trametinib Sy.x
B
hM1F Gemcitabine Sy.x
hM1F Paclitaxel Sy.x
hM1F SN-38 Sy.x
hM1F Oxaliplatin Sy.x
hM1F 5-FU Sy.x
hM1F Trametinib Sy.x
Sy.x (% viability)
0
10
20
30
Matrigel 04 01 - - -
Cultrex - - 83 87 -
Ultimatrix - - - - 96

Figure 3A-B

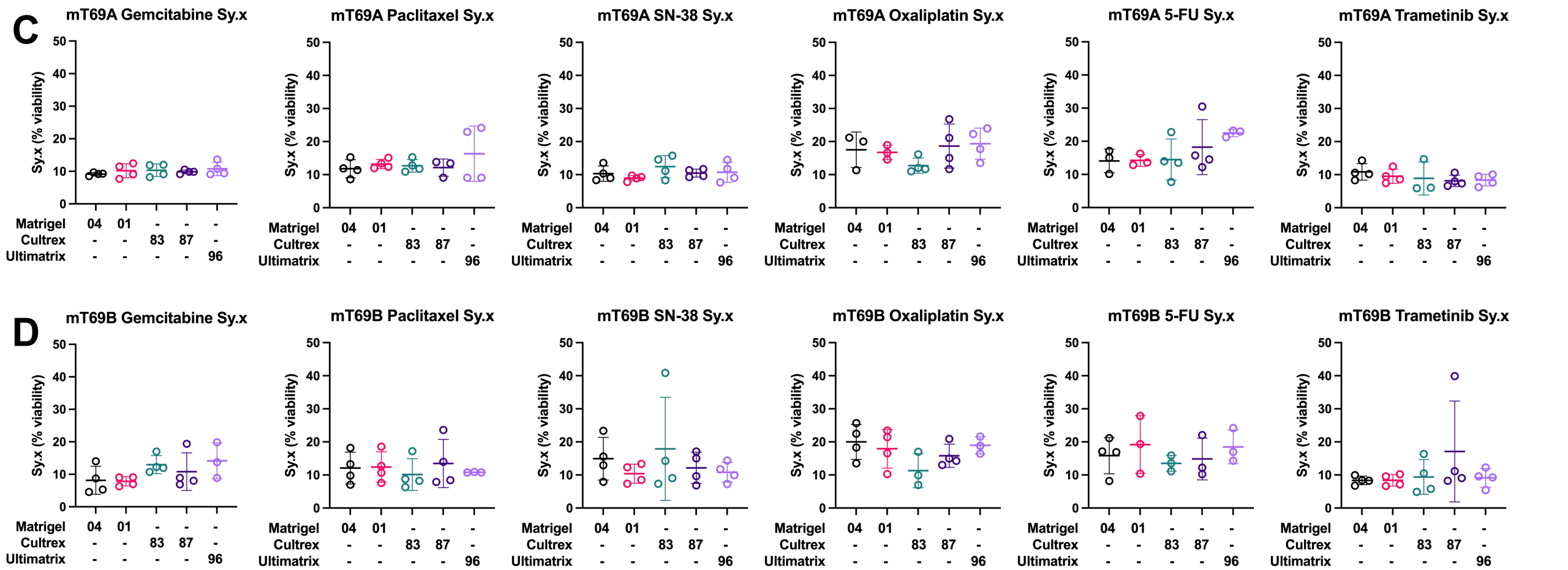
C
mT69A Gemcitabine Sy.x
mT69A Paclitaxel Sy.x
mT69A SN-38 Sy.x
mT69A Oxaliplatin Sy.x
mT69A 5-FU Sy.x
mT69A Trametinib Sy.x
D
mT69B Gemcitabine Sy.x
mT69B Paclitaxel Sy.x
mT69B SN-38 Sy.x
mT69B Oxaliplatin Sy.x
mT69B 5-FU Sy.x
mT69B Trametinib Sy.x
Sy.x (% viability)
0
10
20
30
40
50
Matrigel 04 01 - - -
Cultrex - - 83 87 -
Ultimatrix - - - - 96

Figure 3C-D

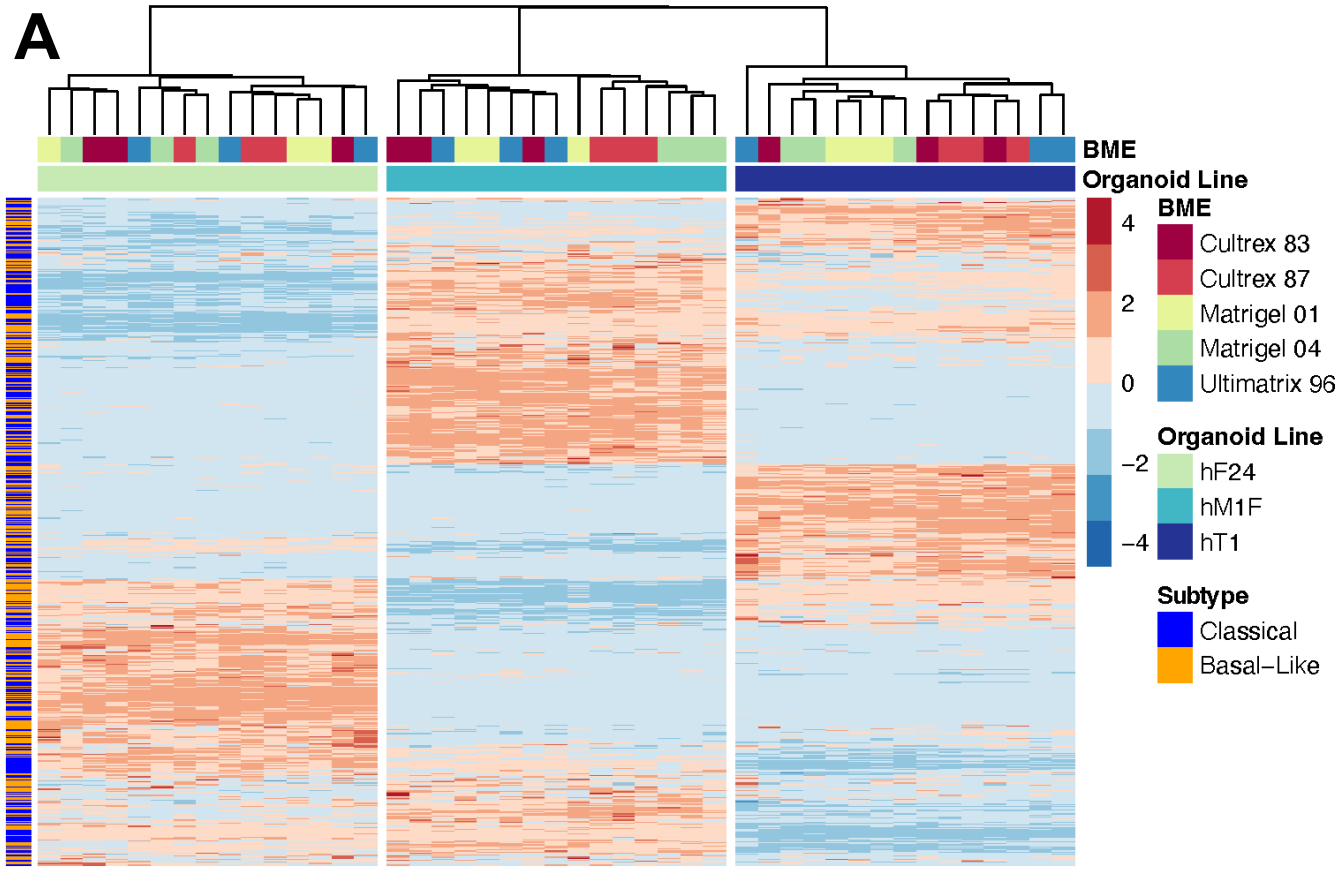
A
BME
Organoid Line
4
2
0
−2
−4
BME
Cultrex 83
Cultrex 87
Matrigel 01
Matrigel 04
Ultimatrix 96
Organoid Line
hF24
hM1F
hT1
Subtype
Classical
Basal−Like

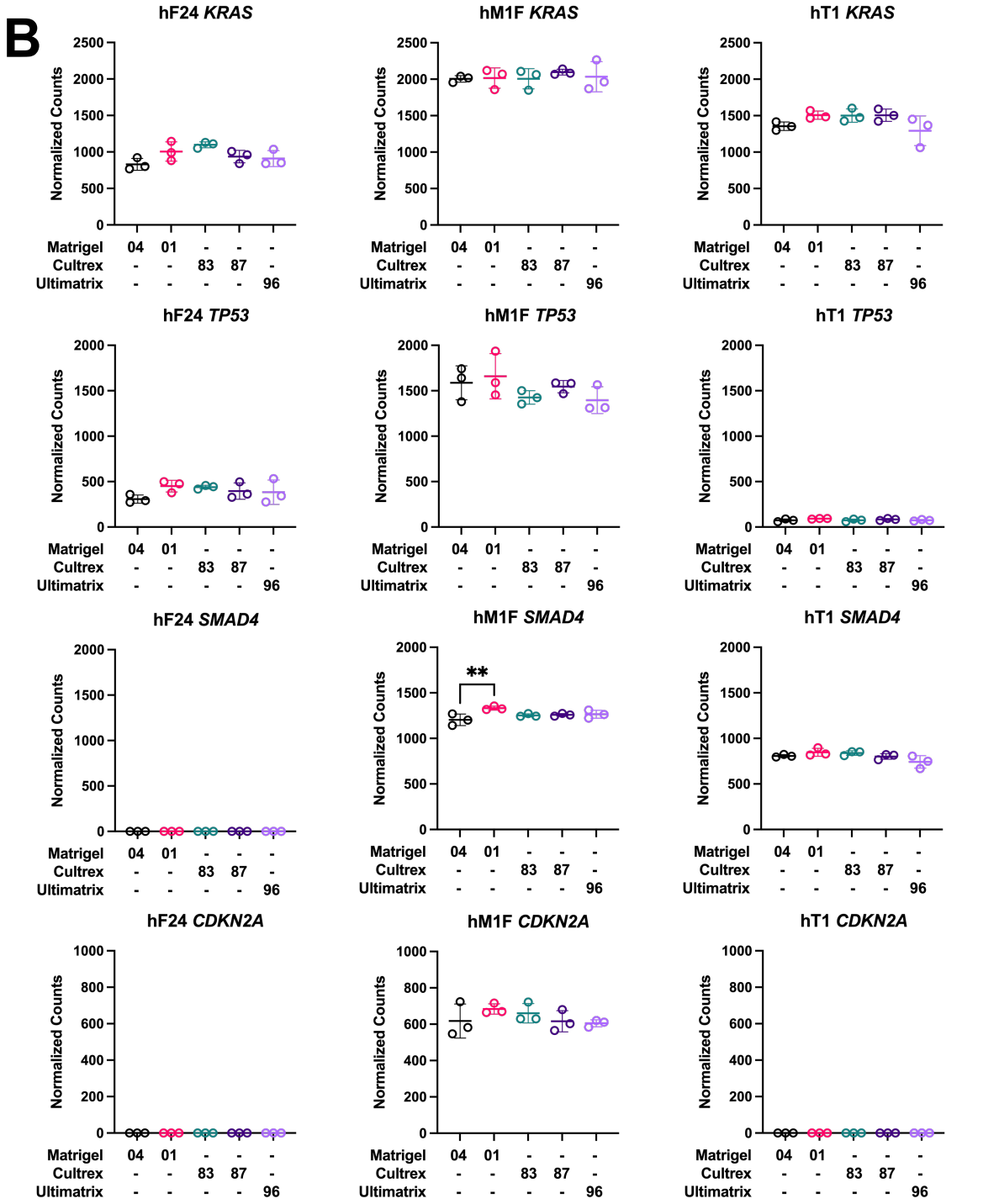
B
hF24 KRAS
hM1F KRAS
hT1 KRAS
hF24 TP53
hM1F TP53
hT1 TP53
hF24 SMAD4
hM1F SMAD4
hT1 SMAD4
hF24 CDKN2A
hM1F CDKN2A
hT1 CDKN2A
Normalized Counts
**
Matrigel 04 01 - - -
Cultrex - - 83 87 -
Ultimatrix - - - - 96

Figure 4

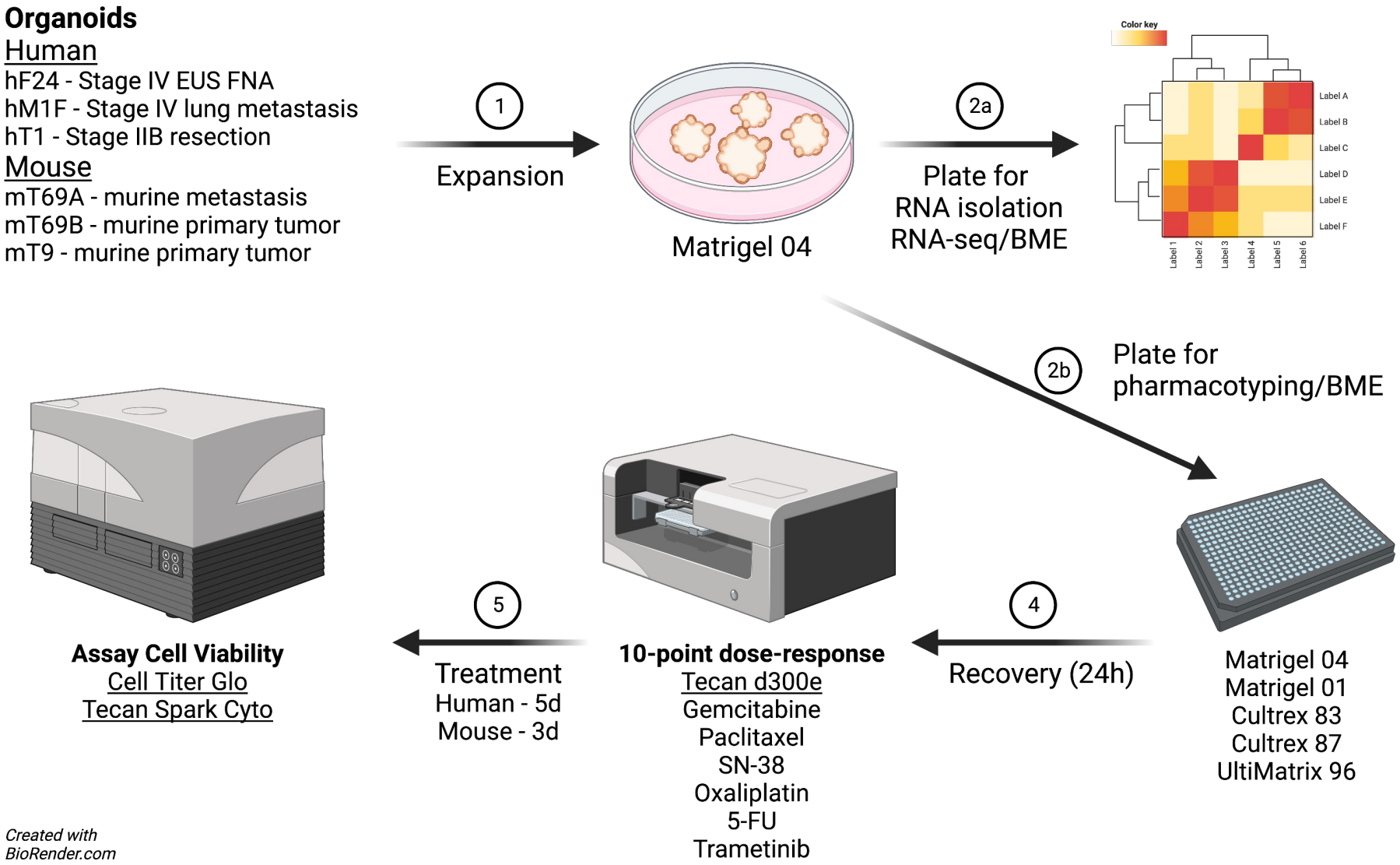

Supplementary Figure 1

Supplementary Table 1

PDO	Origin	Site	Type of sample	Sex	Age	Race	Stage	KRAS (allele frequencies)	TP53 (allele frequencies)	SMAD4 (allele frequencies)	CDKN2A (allele frequencies)
hF24*	H. sapiens	Pancreas	EUS FNA	F	57	Caucasian	4	G12V 82%	F113V (100%)	LOSS (N/A)	DEEP LOSS (N/A)
hM1F*	H. sapiens	Lung	RAP	M	55	Caucasian	4	G12D 73%	R175H (100%)	WT (N/A)	WT (N/A)
hT1*	H. sapiens	Pancreas	Resection	M	65	Caucasian	2B	G12V 39%	R213* (100%)	WT (N/A)	DEEP LOSS (N/A)

*H. Tiriac *et al.*, Organoid Profiling Identifies Common Responders to Chemotherapy in Pancreatic Cancer. *Cancer Discov* **8**, 1112-1129 (2018).

Supplementary Table 2

PDO	Origin	Sex	Site	Type of sample
mT69A	M. musculus	F	Pancreas	KPC B6, PDAC local pancreatic metastasis
mT69B	M. musculus	F	Pancreas	KPC B6, PDAC primary tumor
mT9	M. musculus	F	Pancreas	KPC PDAC primary tumor

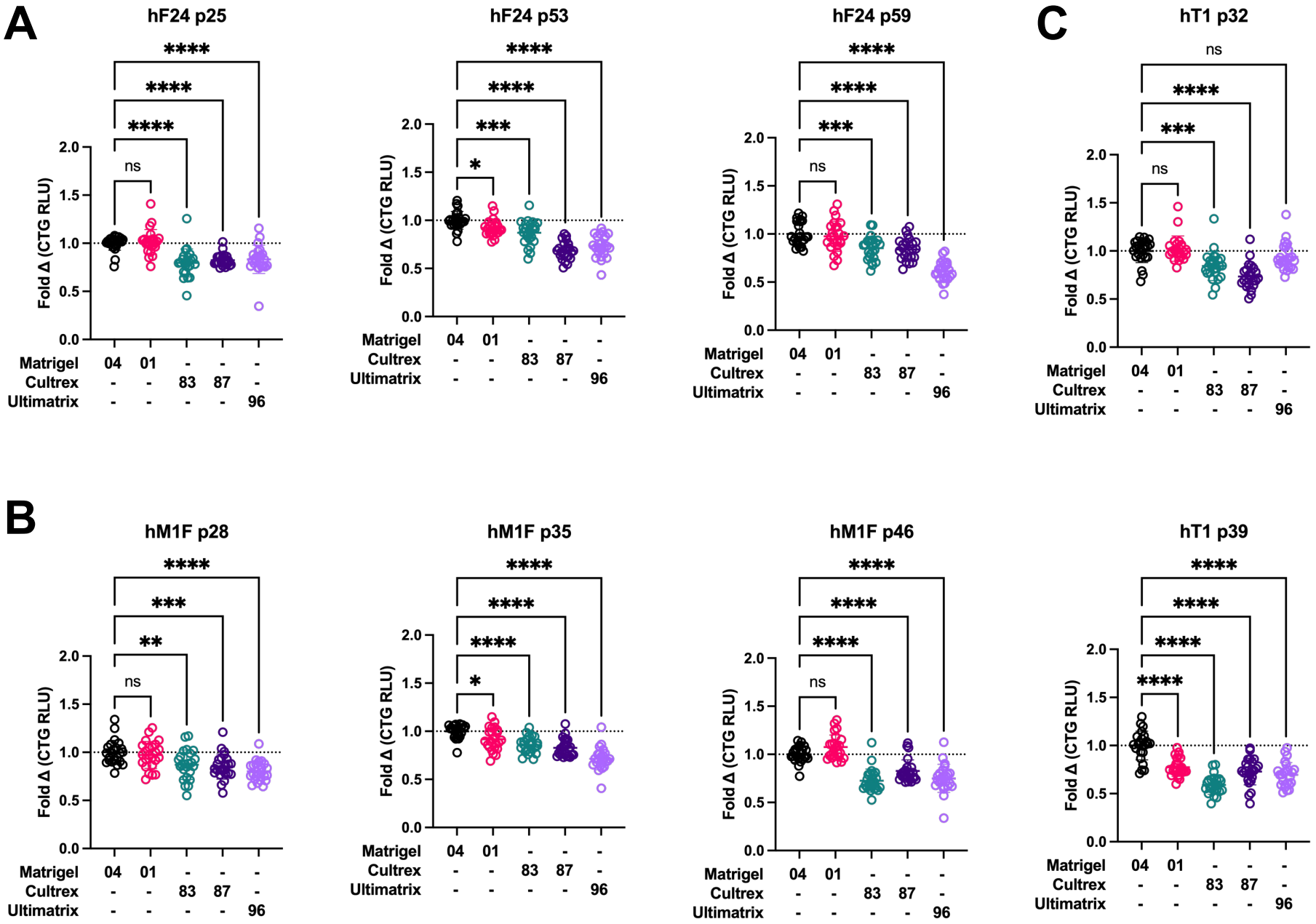

Supplementary Figure 2A-C

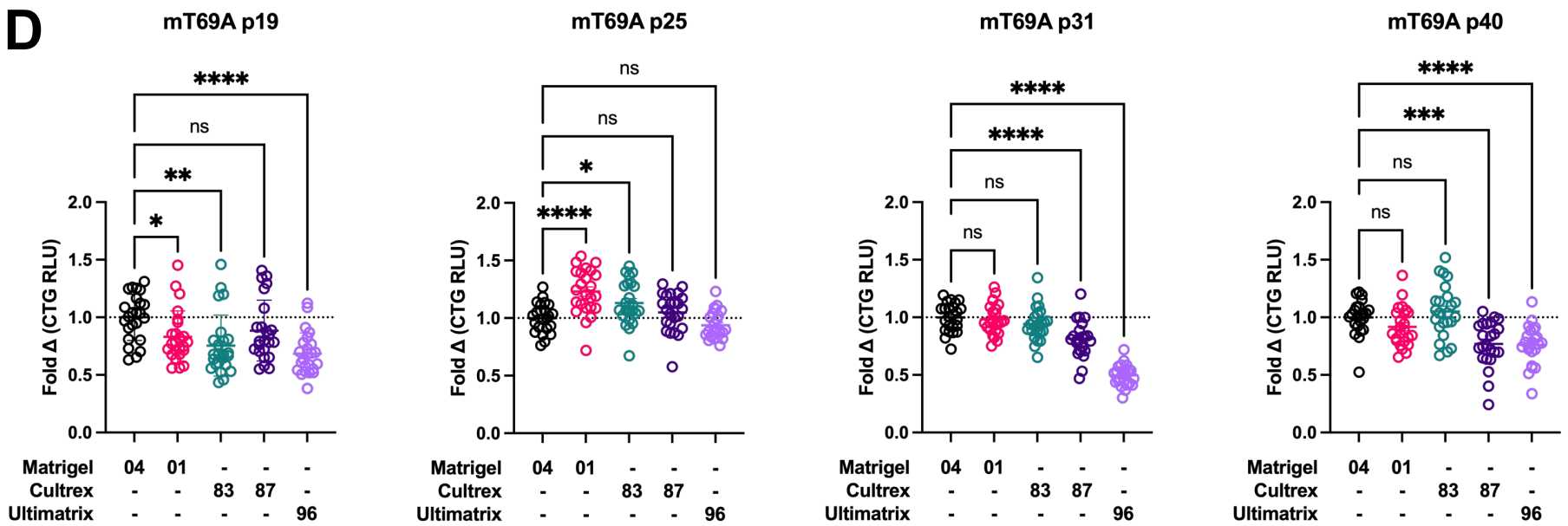

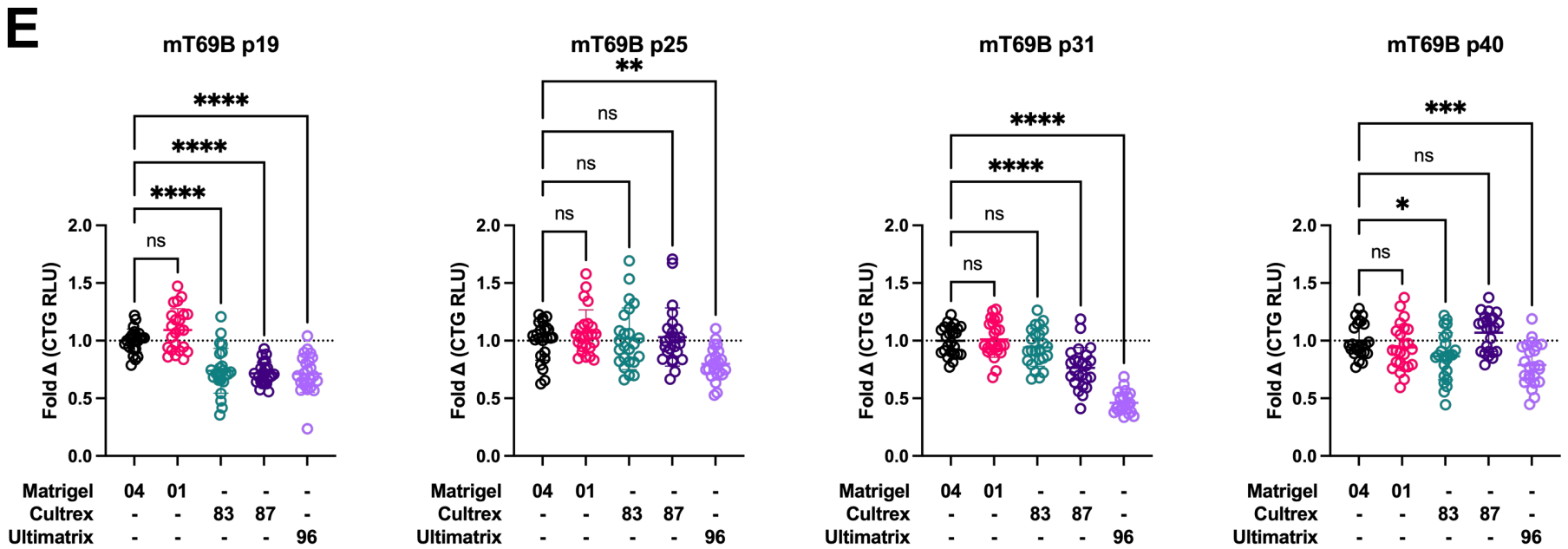

Supplementary Figure 2D-E

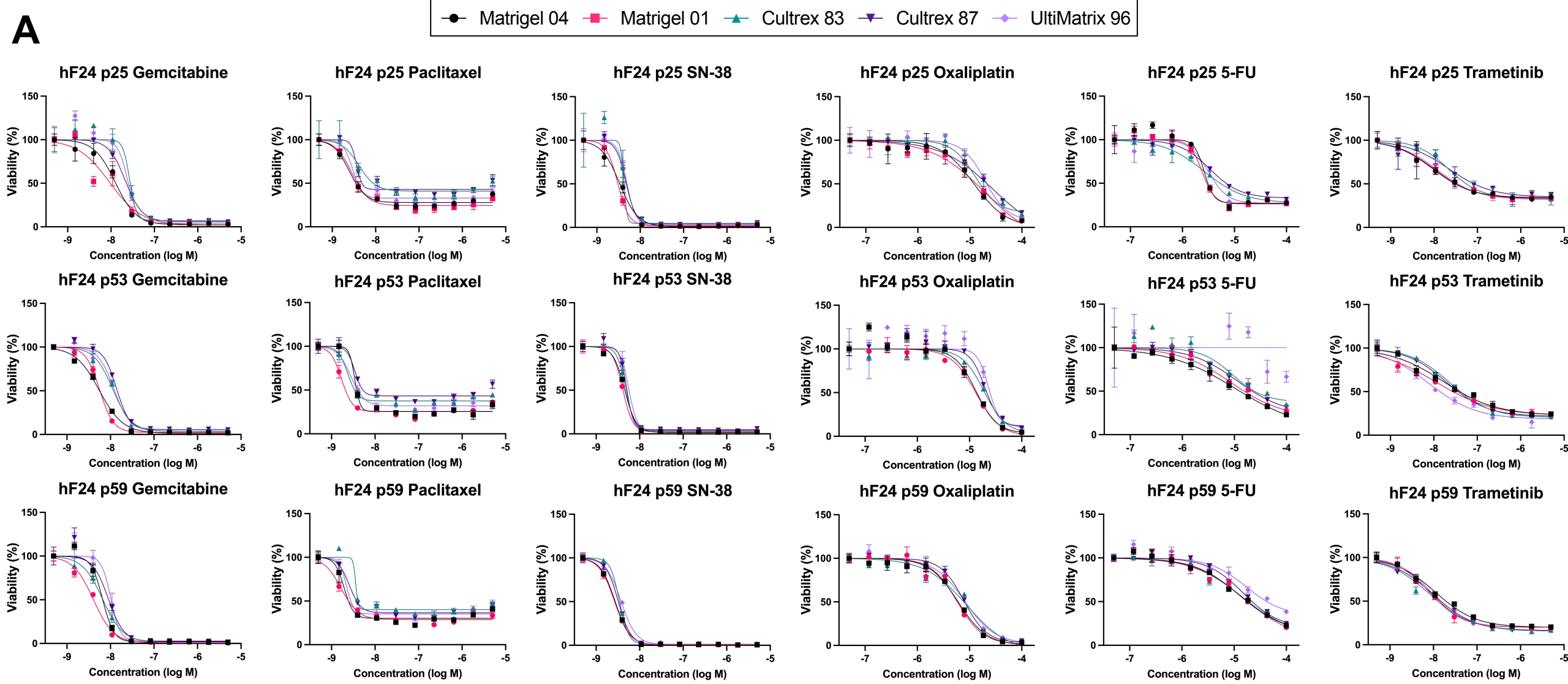

Supplementary Figure 3A

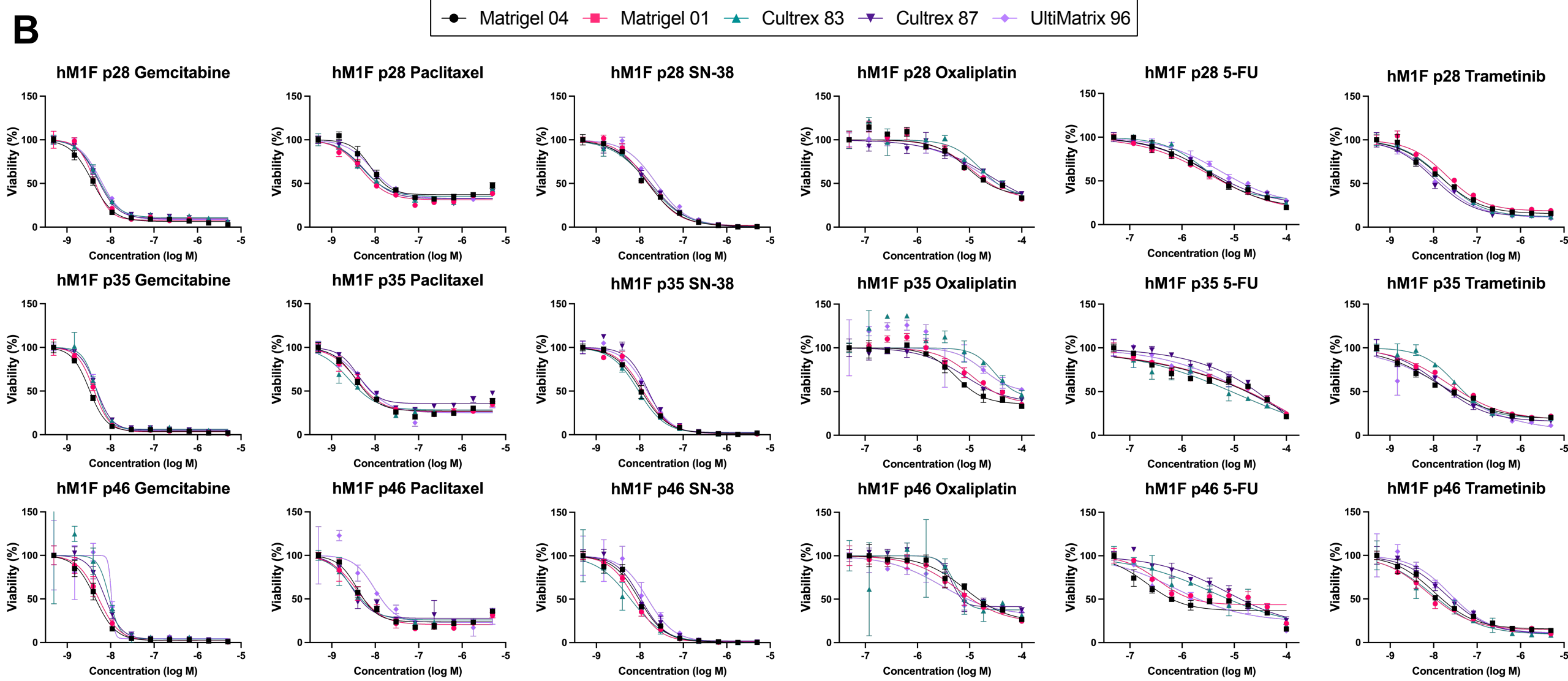

Supplementary Figure 3B

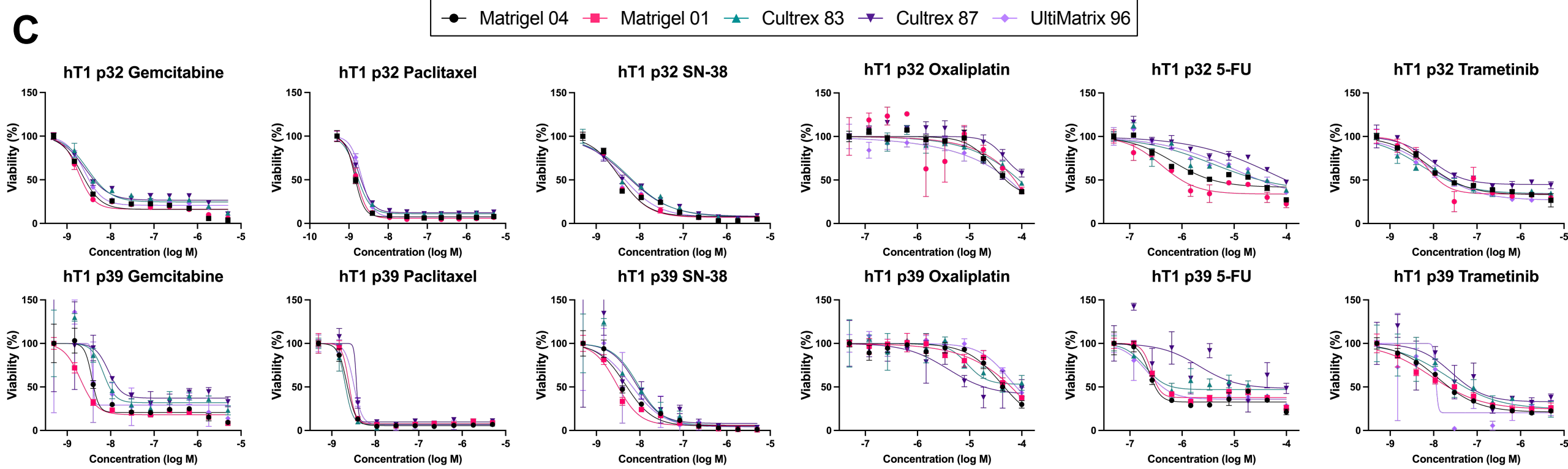

Supplementary Figure 3C

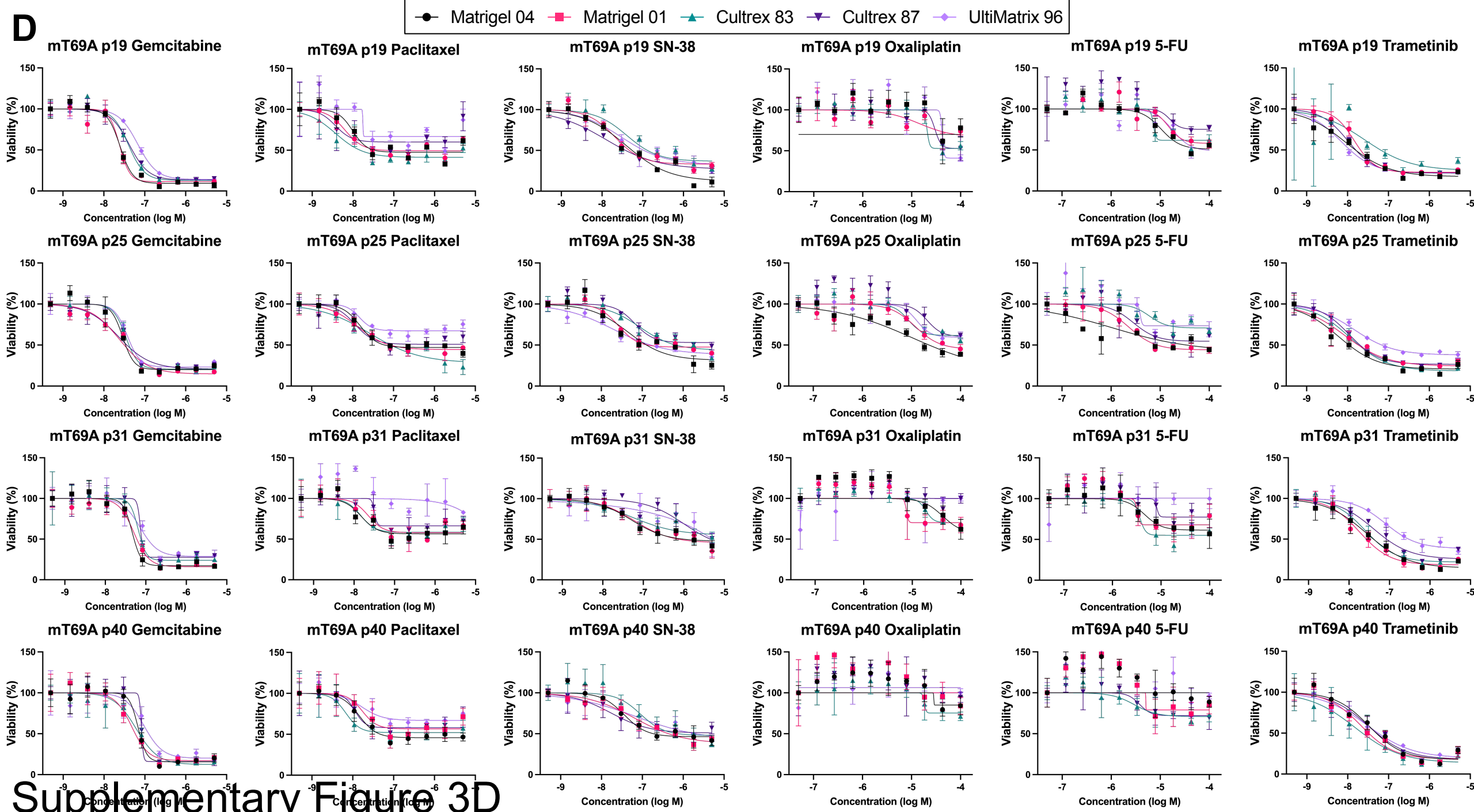

Supplementary Figure 3D

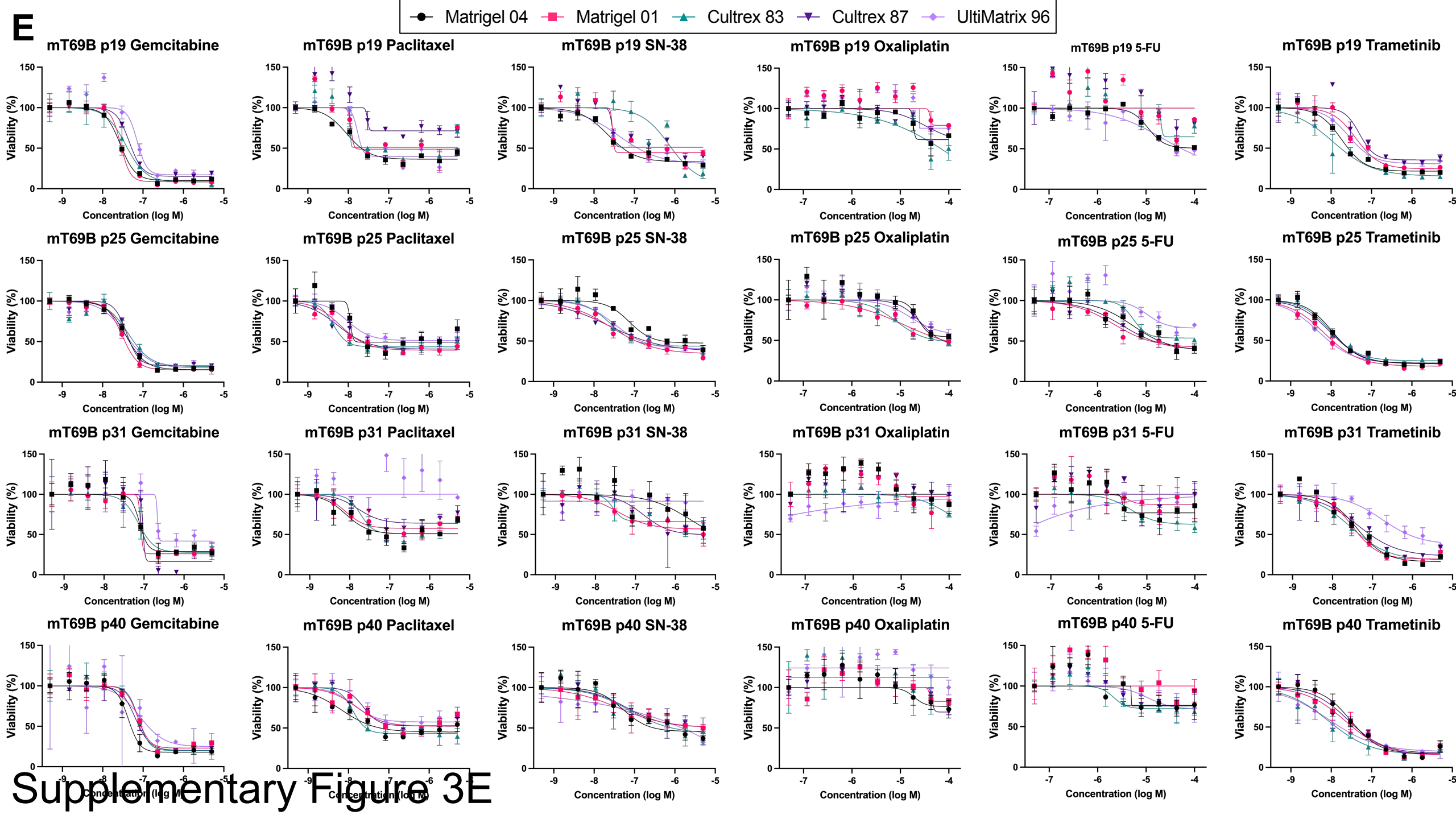

Supplementary Figure 3E

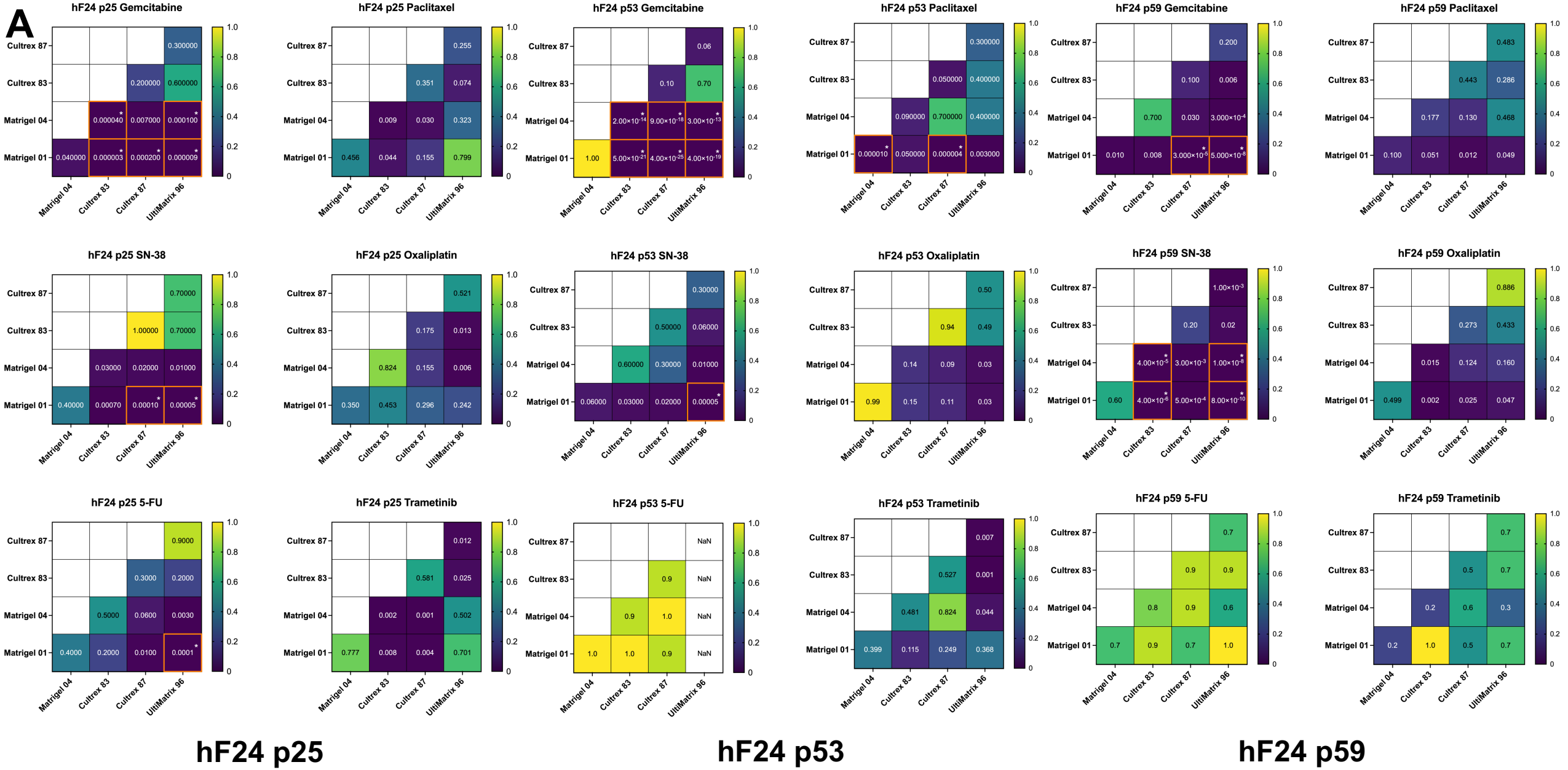

Supplementary Figure 4A – IC50

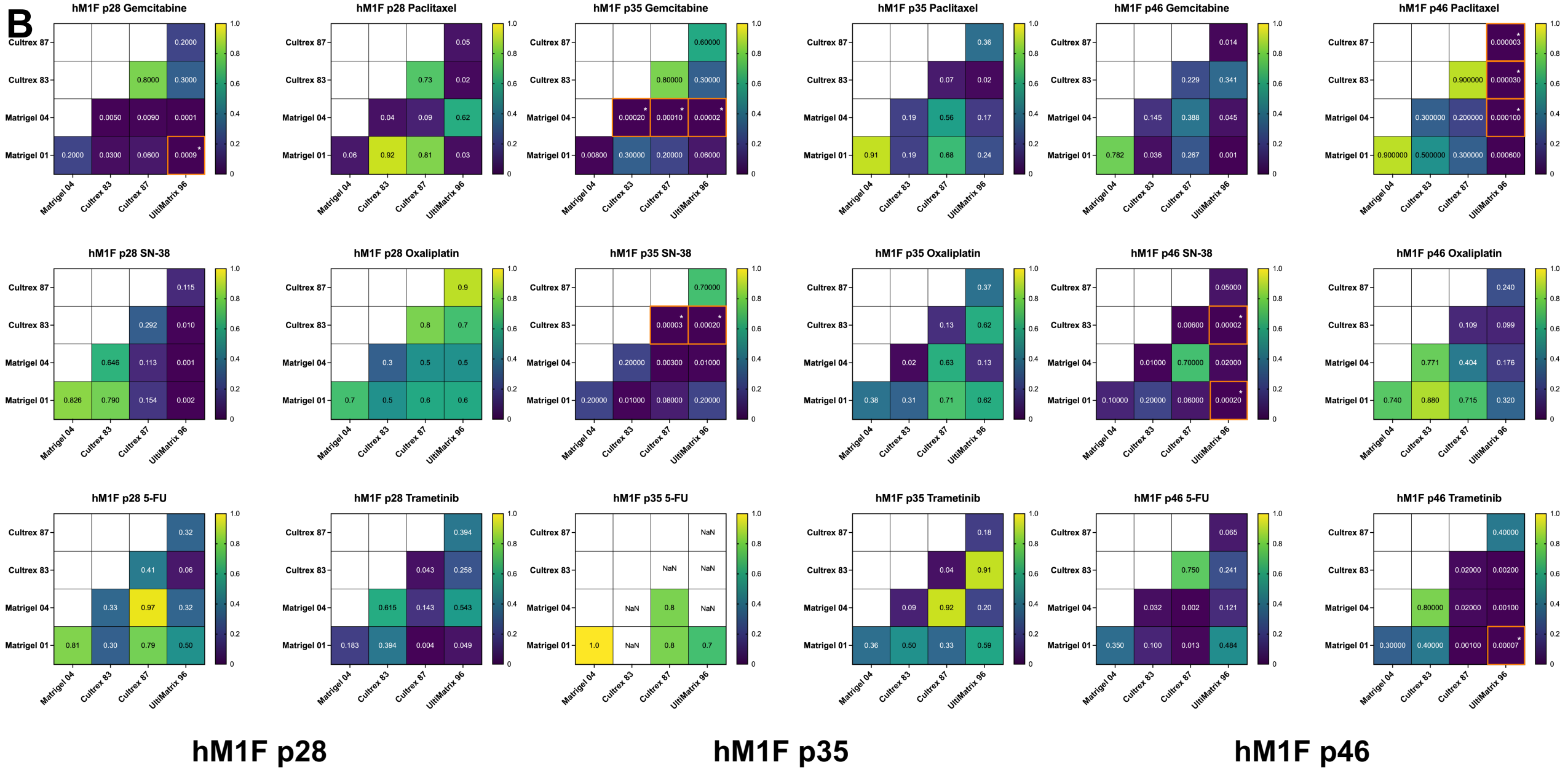

Supplementary Figure 4B – IC50

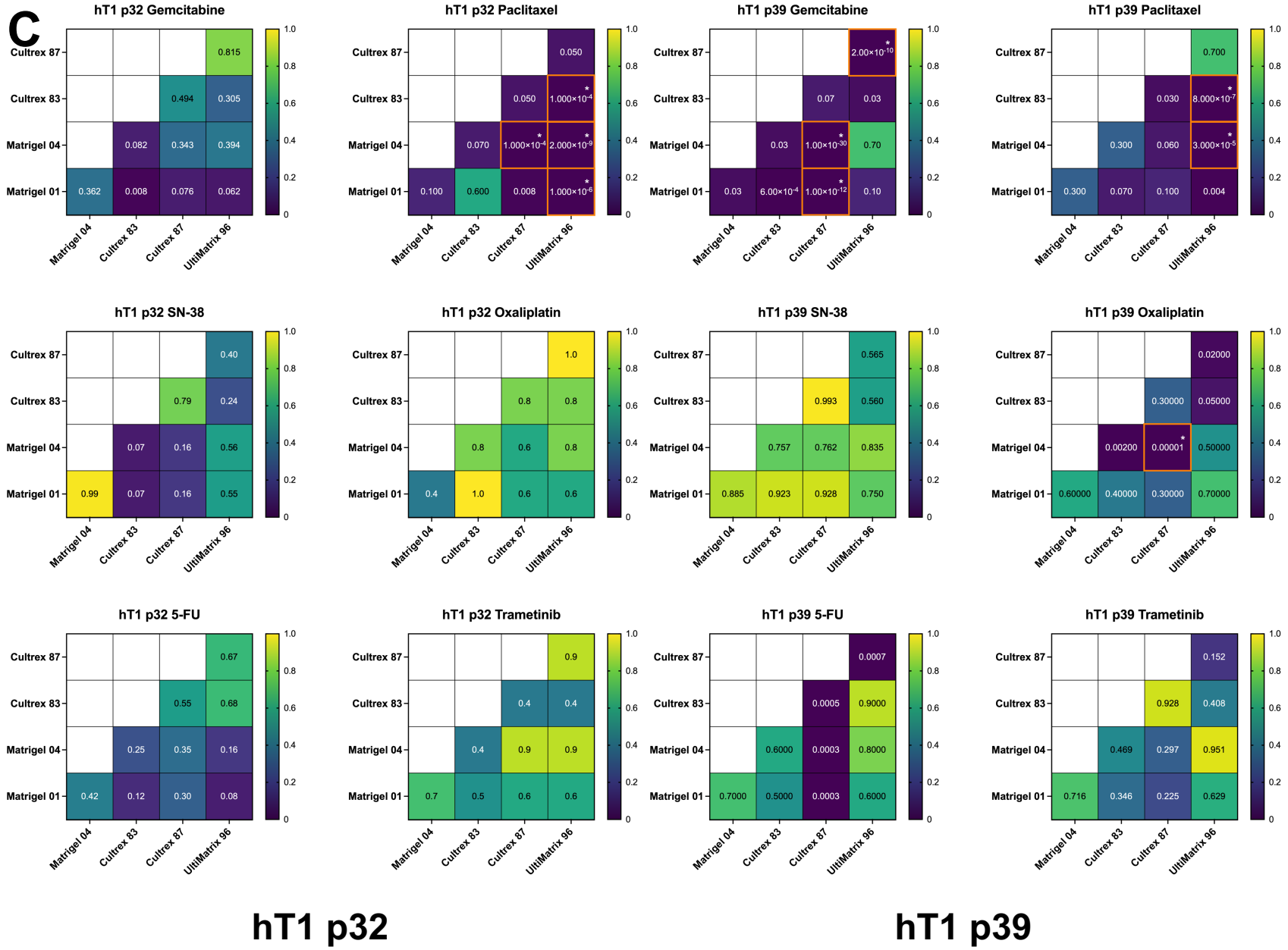

Supplementary Figure 4C – IC50

D

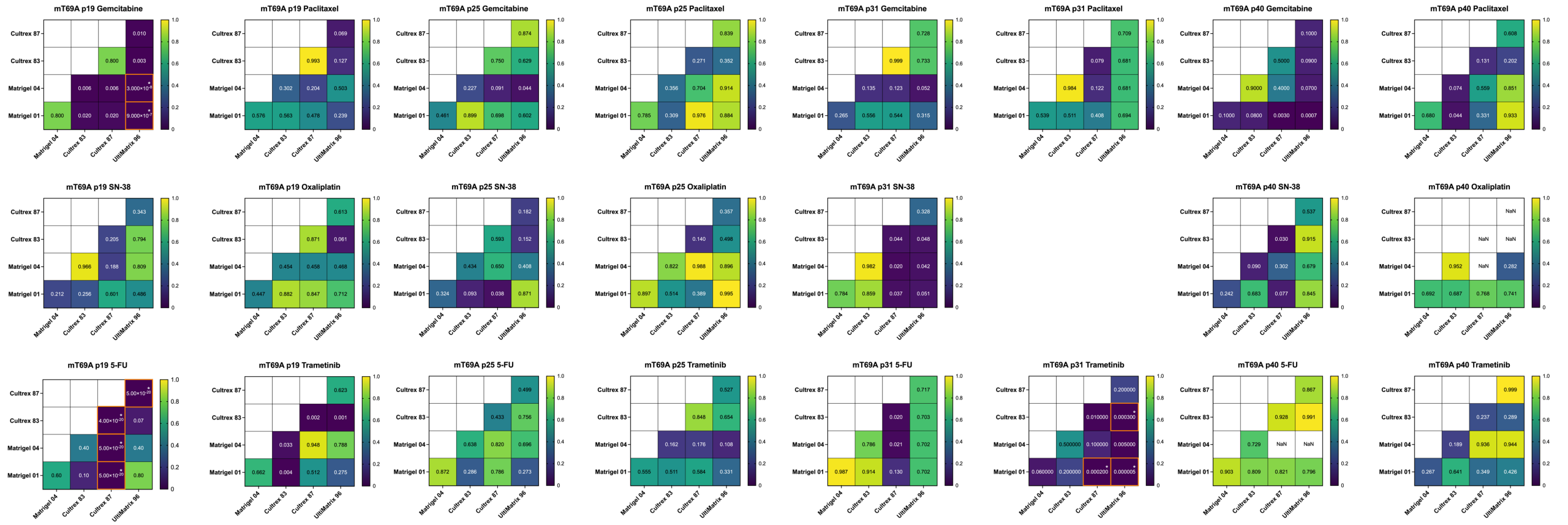

mT69A p19 **mT69A p25** **mT69A p31** **mT69A p40**

Supplementary Figure 4D – IC50

E

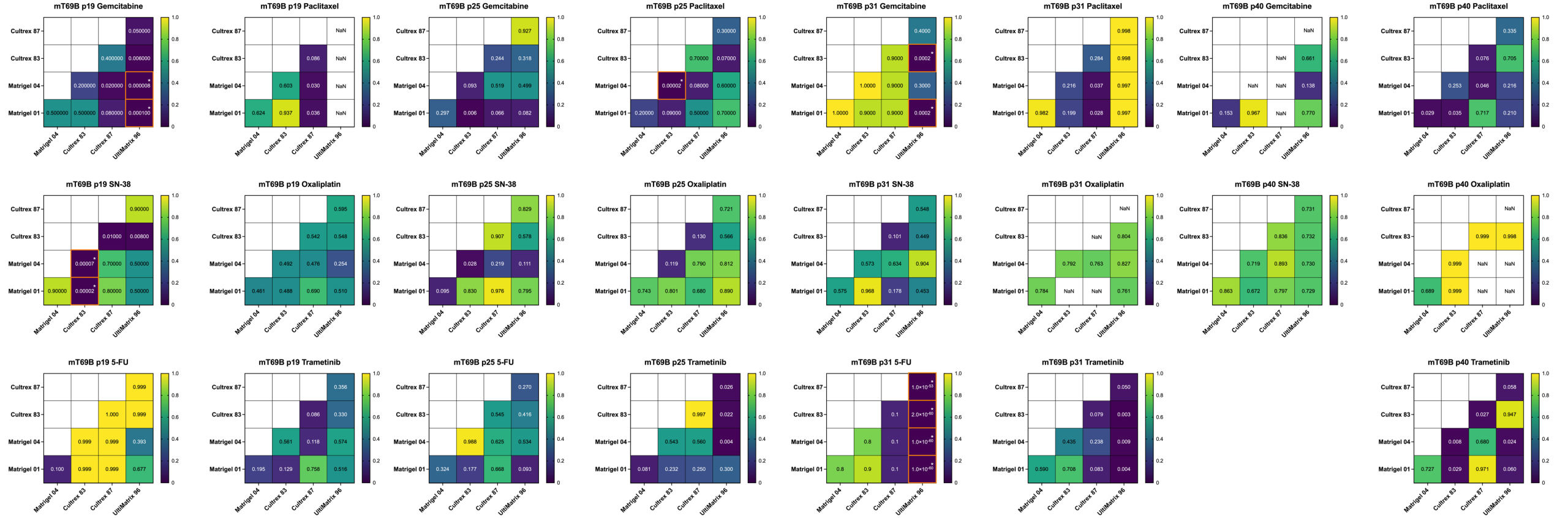

mT69B p19 **mT69B p25** **mT69B p31** **mT69B p40**

Supplementary Figure 4E – IC50

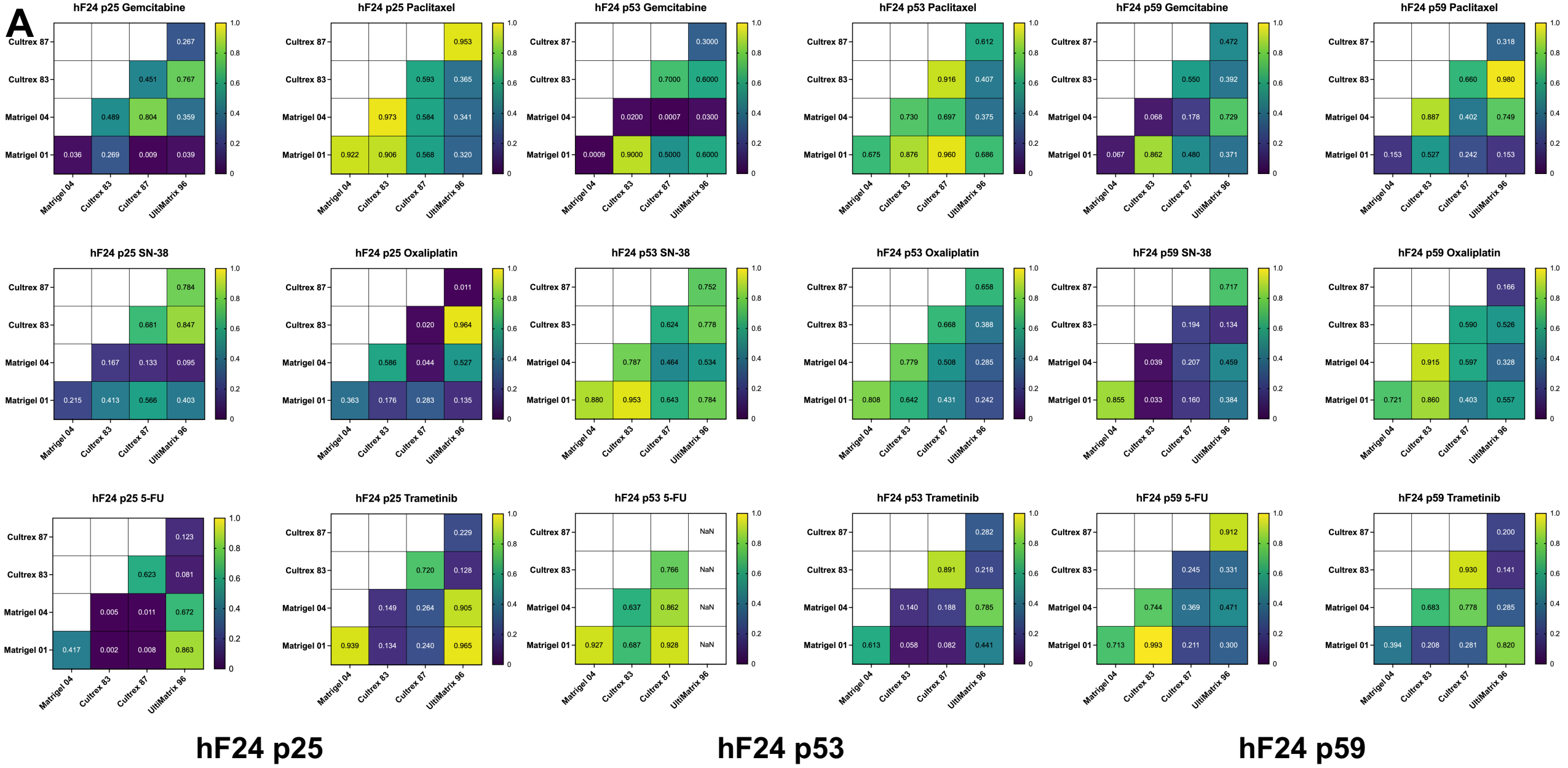

Supplementary Figure 5A – Hill Slope

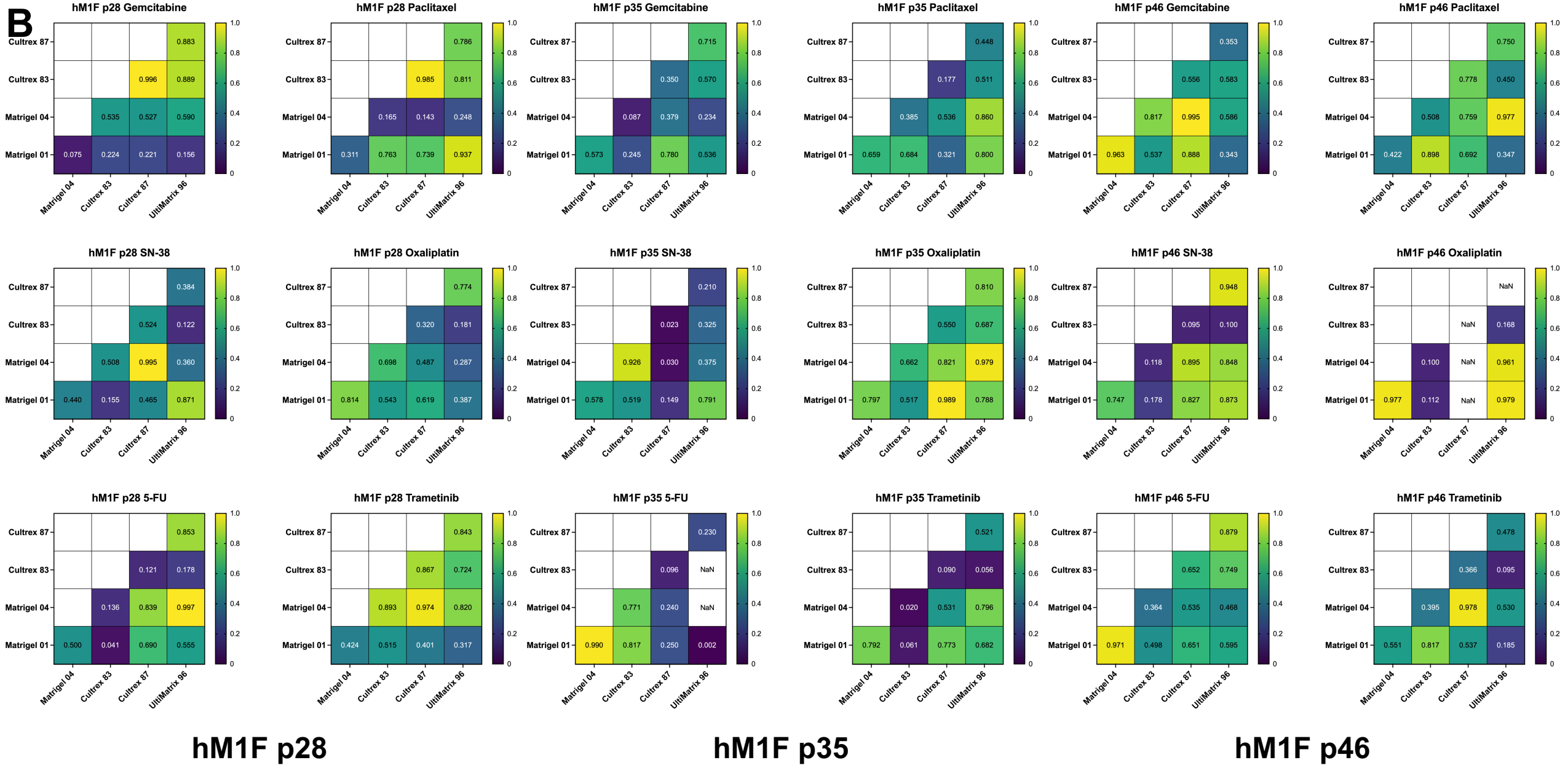

Supplementary Figure 5B – Hill Slope

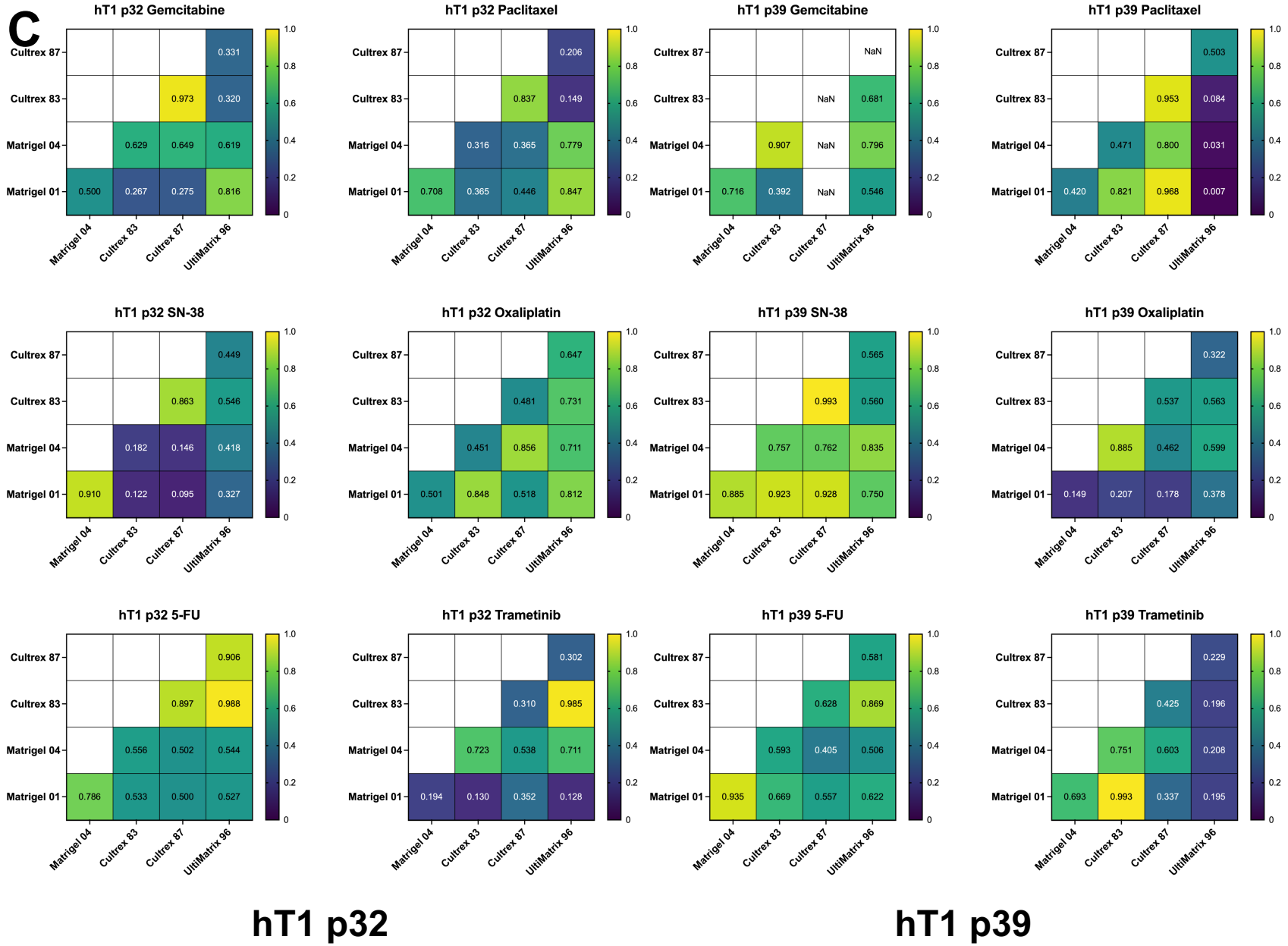

Supplementary Figure 5C – Hill Slope

D

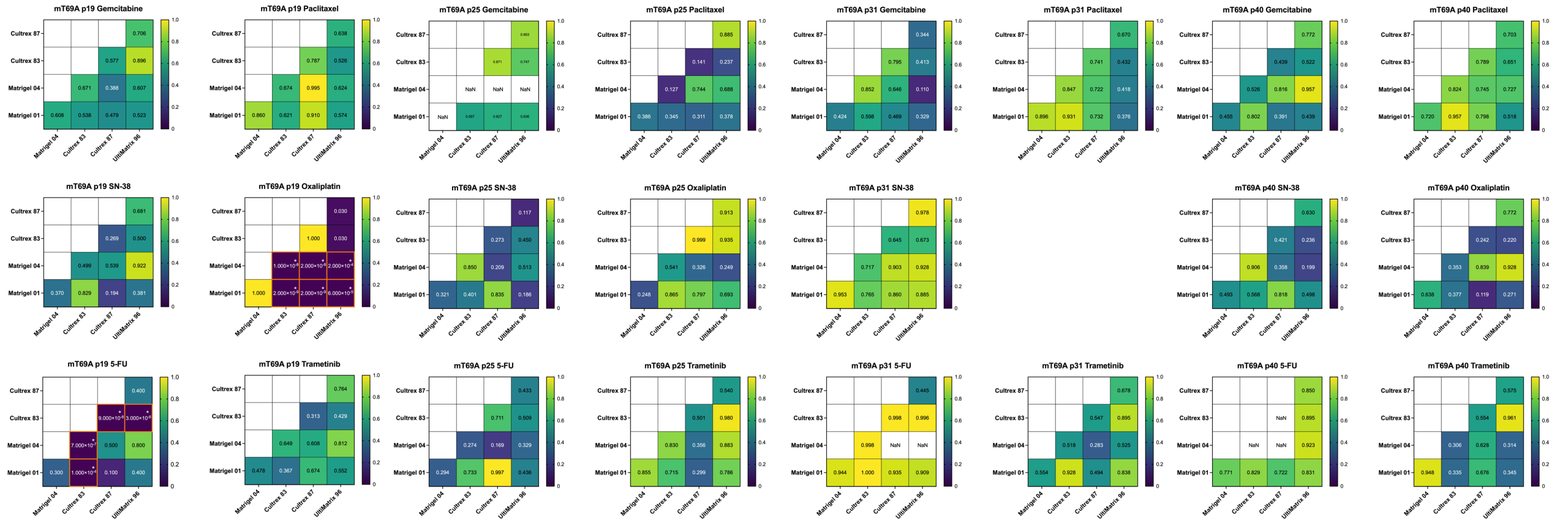

mT69A p19 **mT69A p25** **mT69A p31** **mT69A p40**

Supplementary Figure 5D – Hill Slope

E

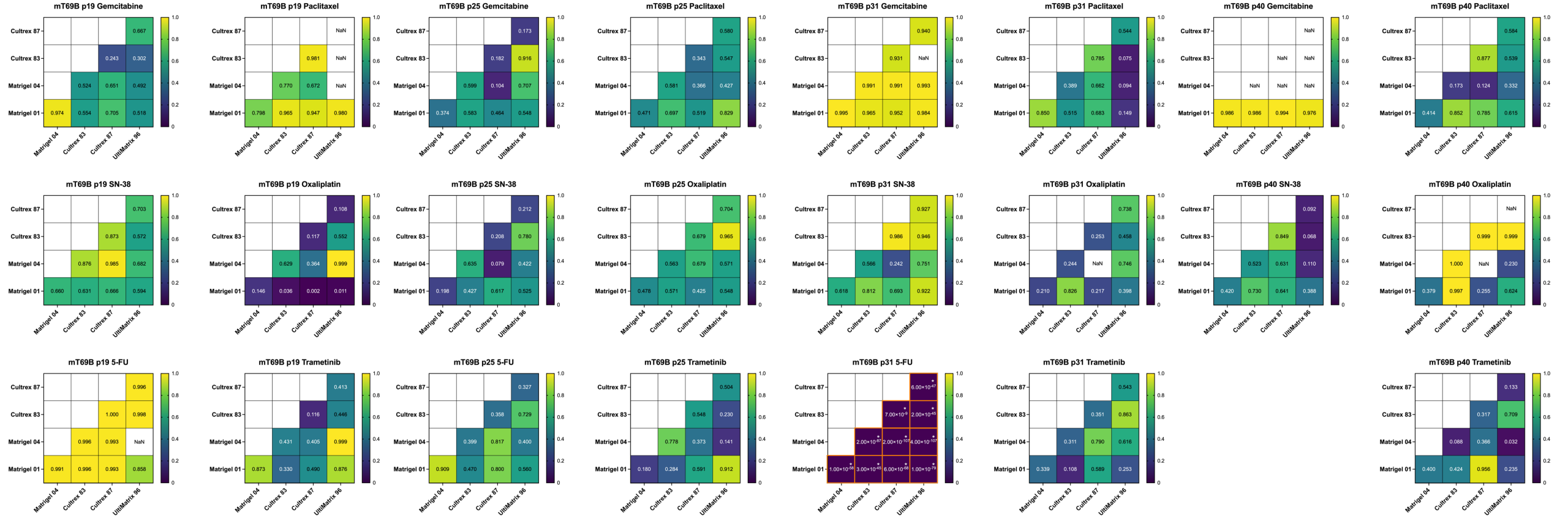

mT69B p19 **mT69B p25** **mT69B p31** **mT69B p40**

Supplementary Figure 5E – Hill Slope

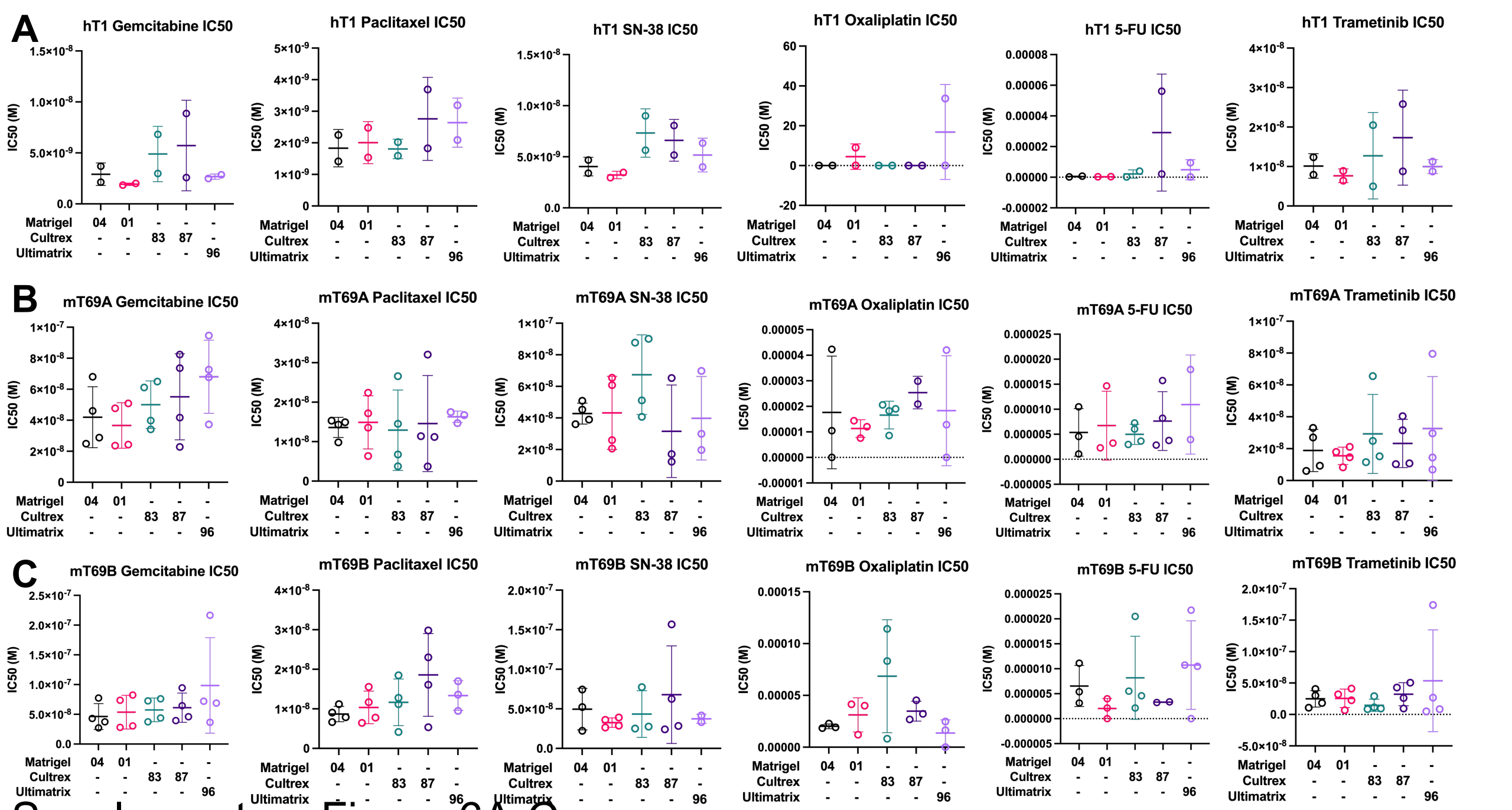

Supplementary Figure 6A-C

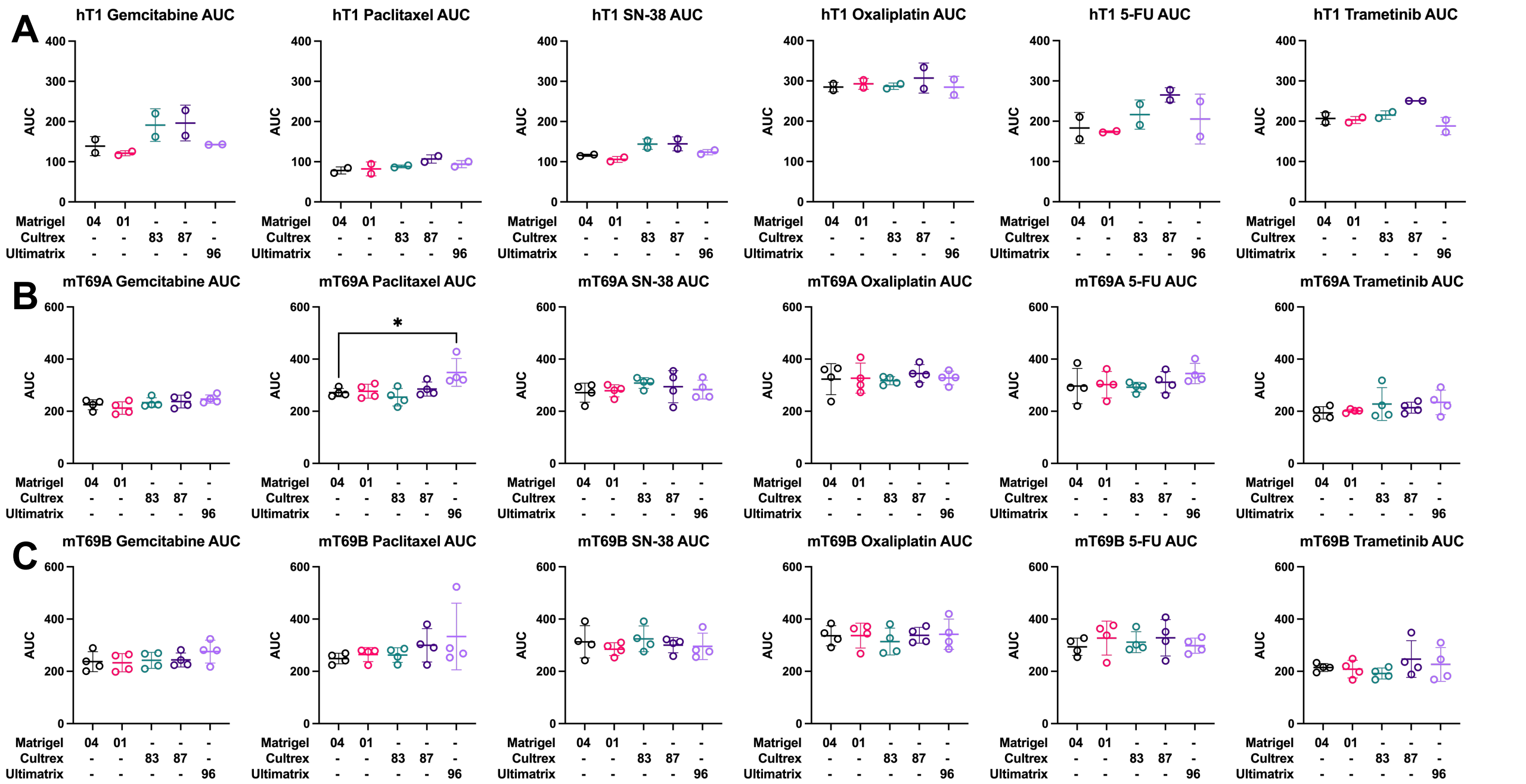

Supplementary Figure 7A-C

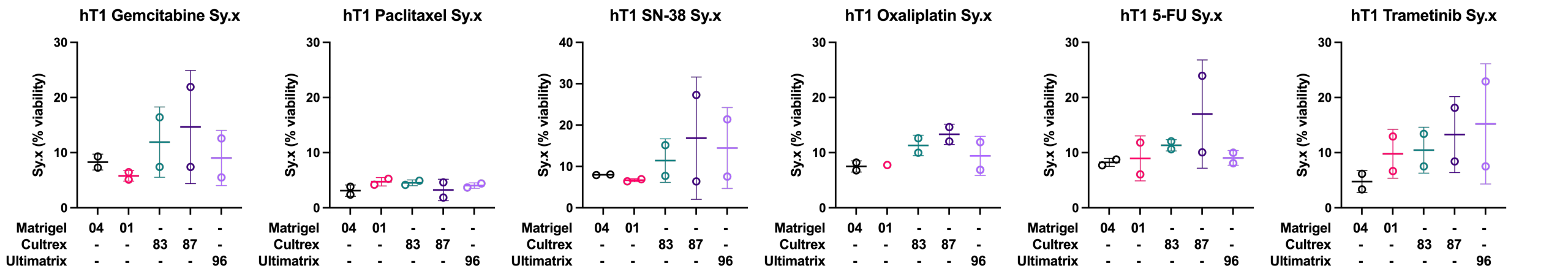

Supplementary Figure 8

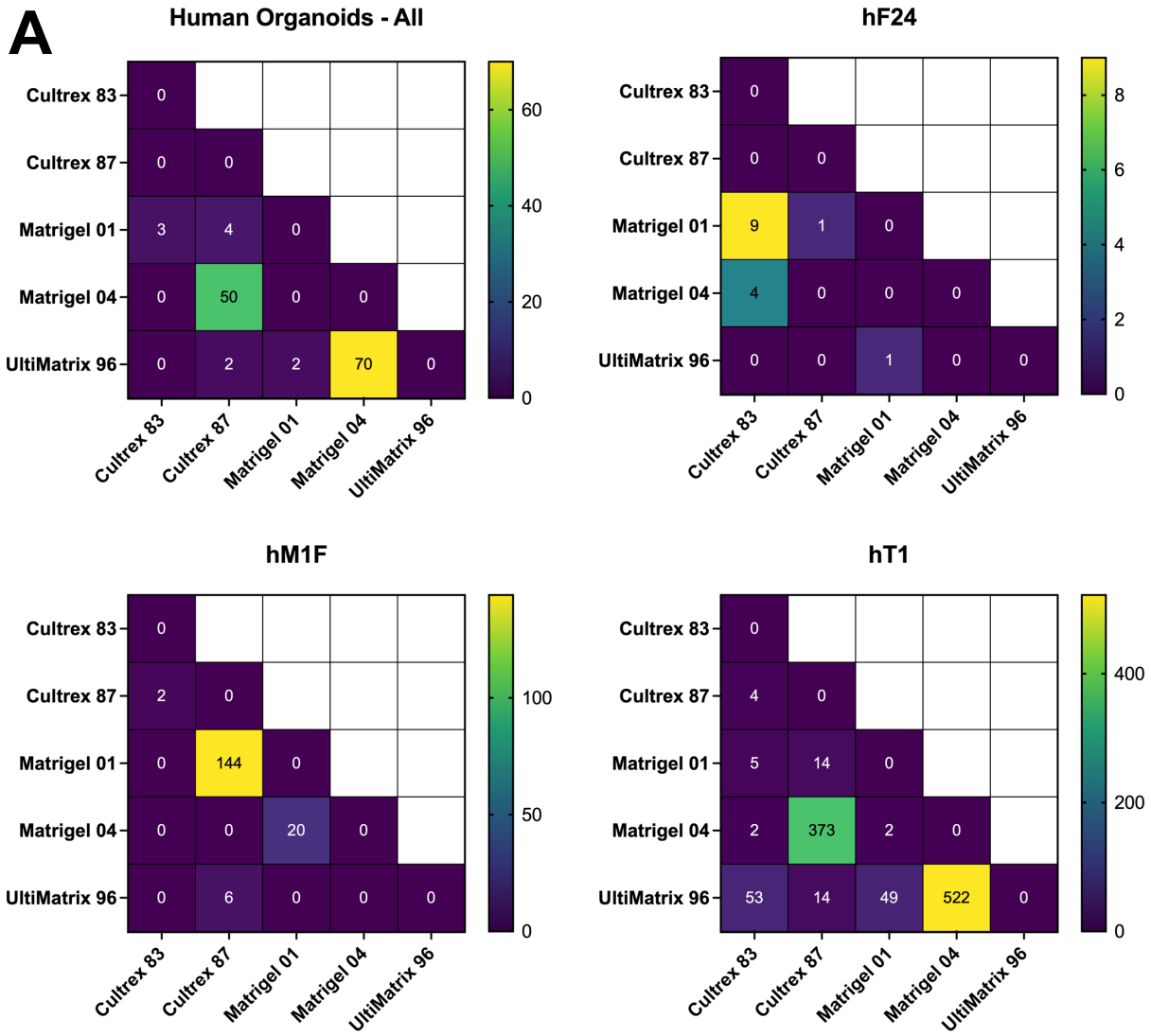

Cells labeled by number of differentially expressed genes (abs(lfc)>1 and FDR ≤ 0.05

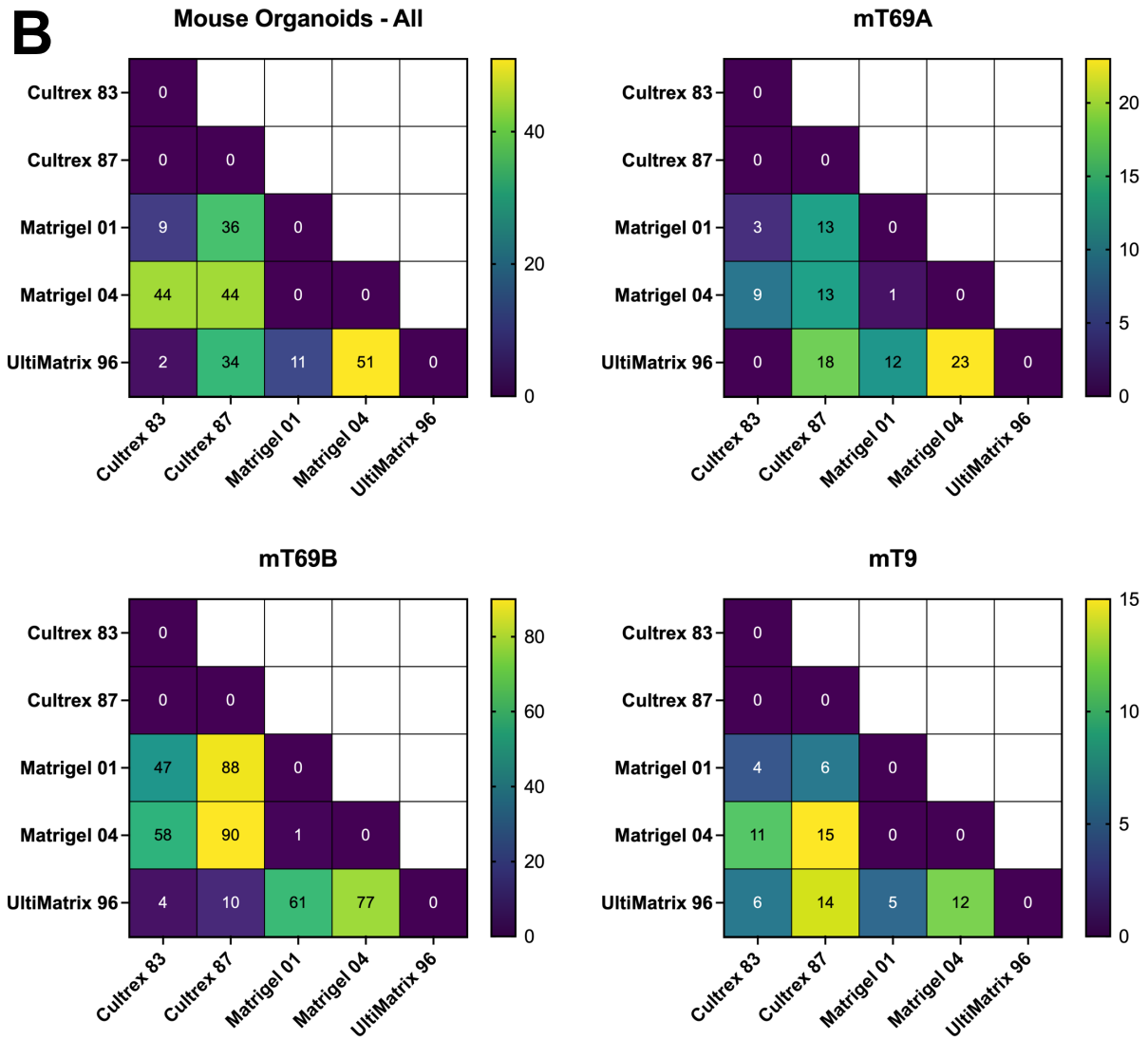

Cells labeled by number of differentially expressed genes (abs(lfc)>1 and FDR ≤ 0.05

Supplementary Figure 9A-B

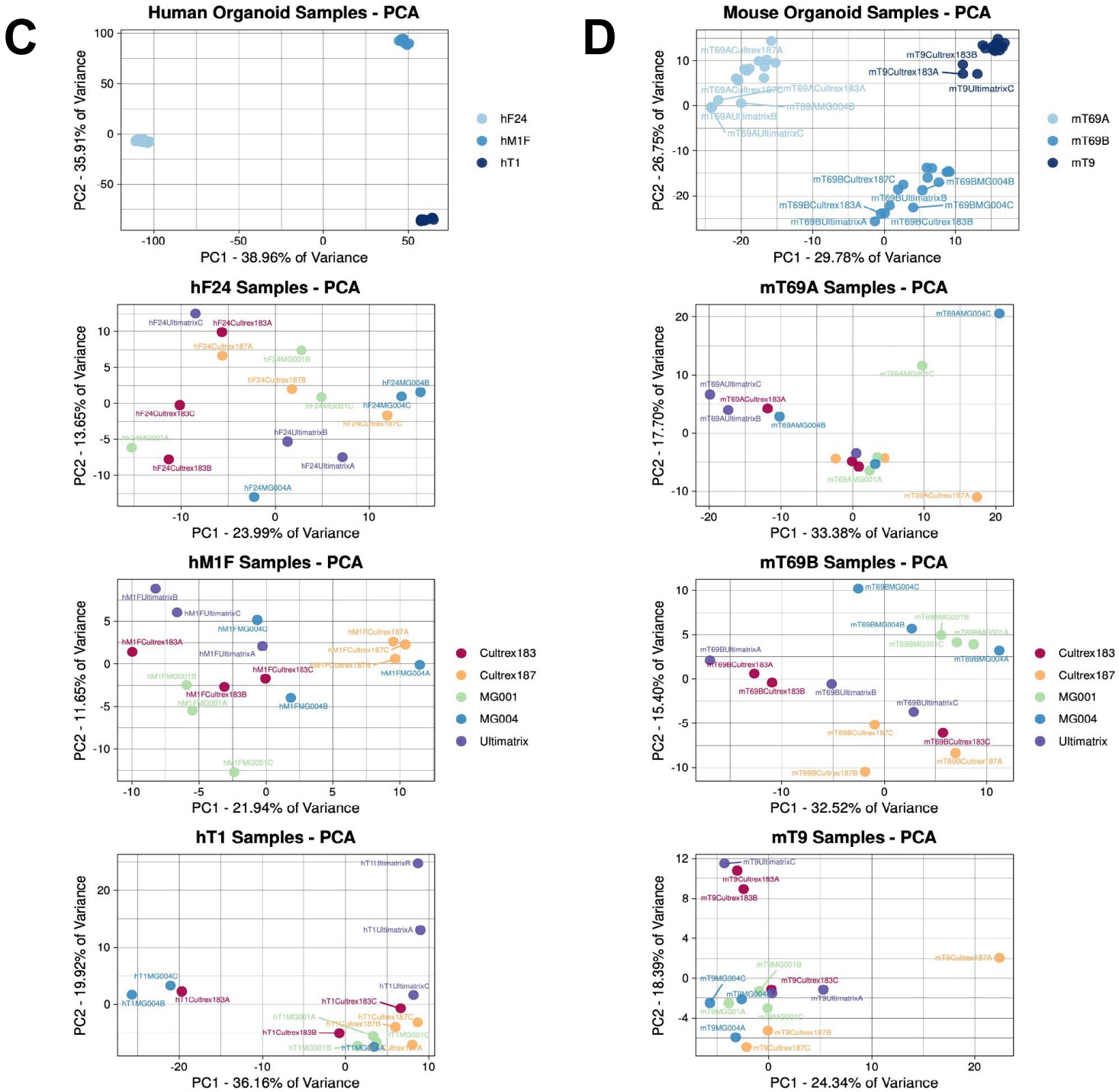

Supplementary Figure 9C-D

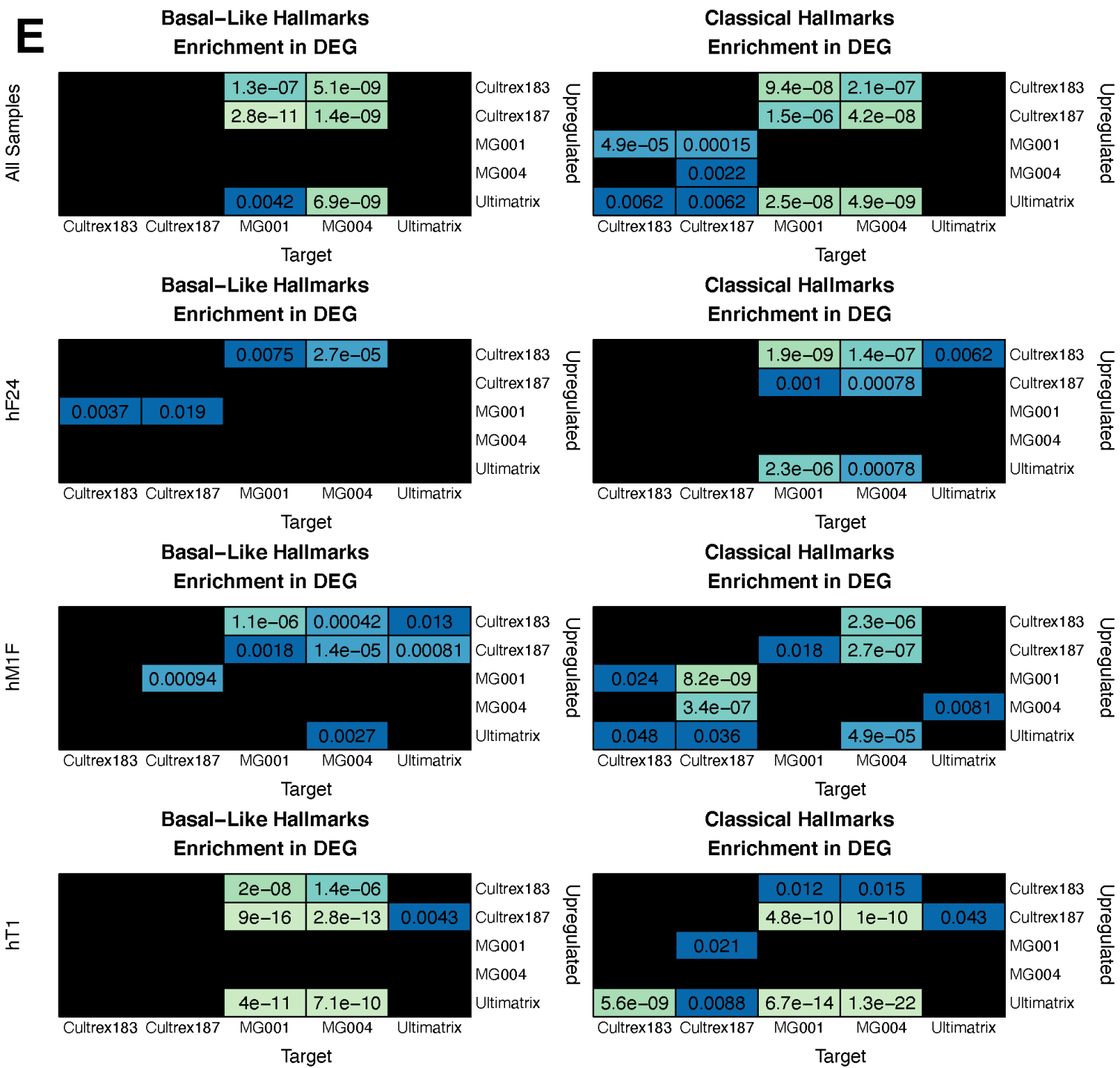

Supplementary Figure 9E

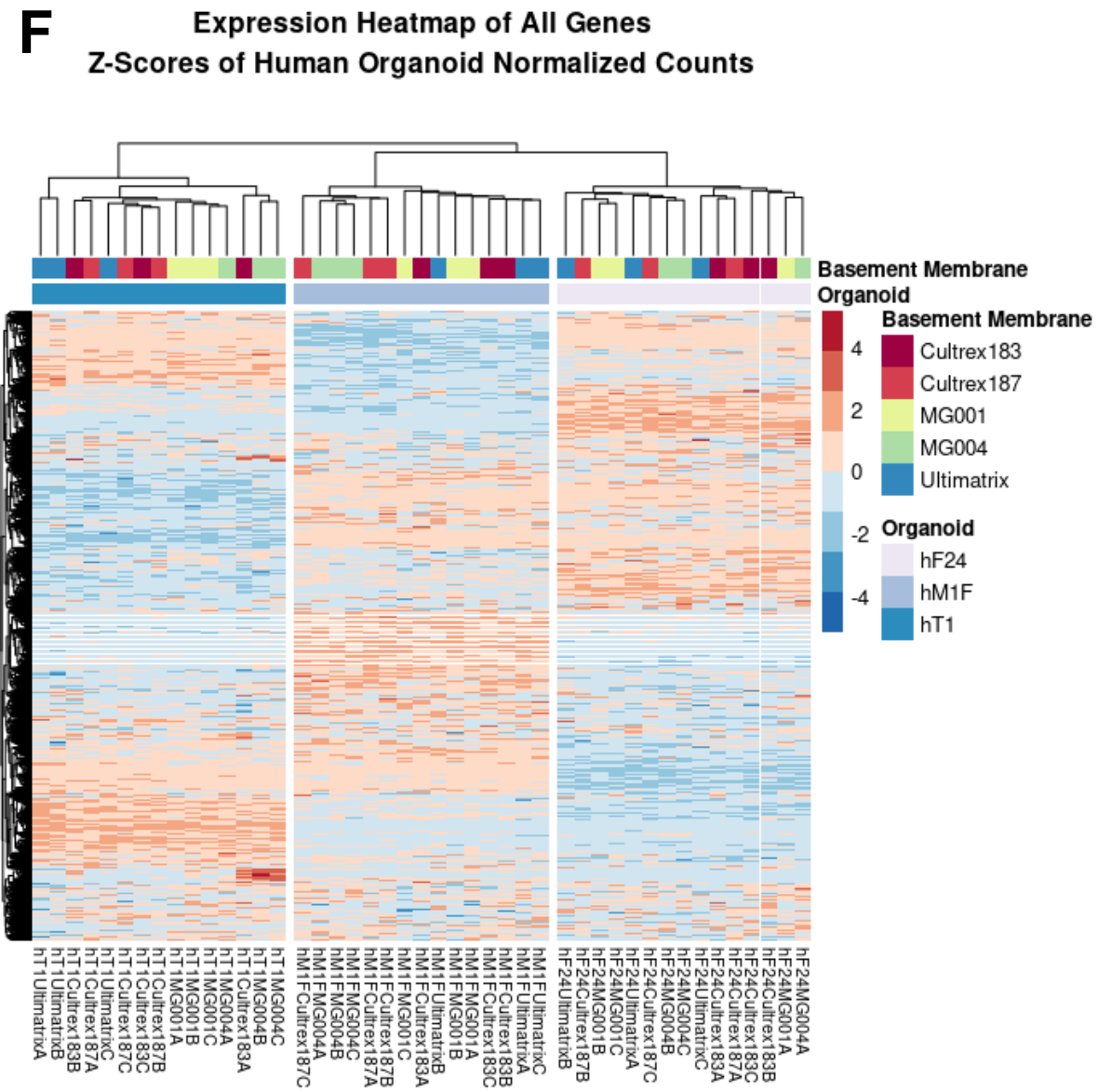

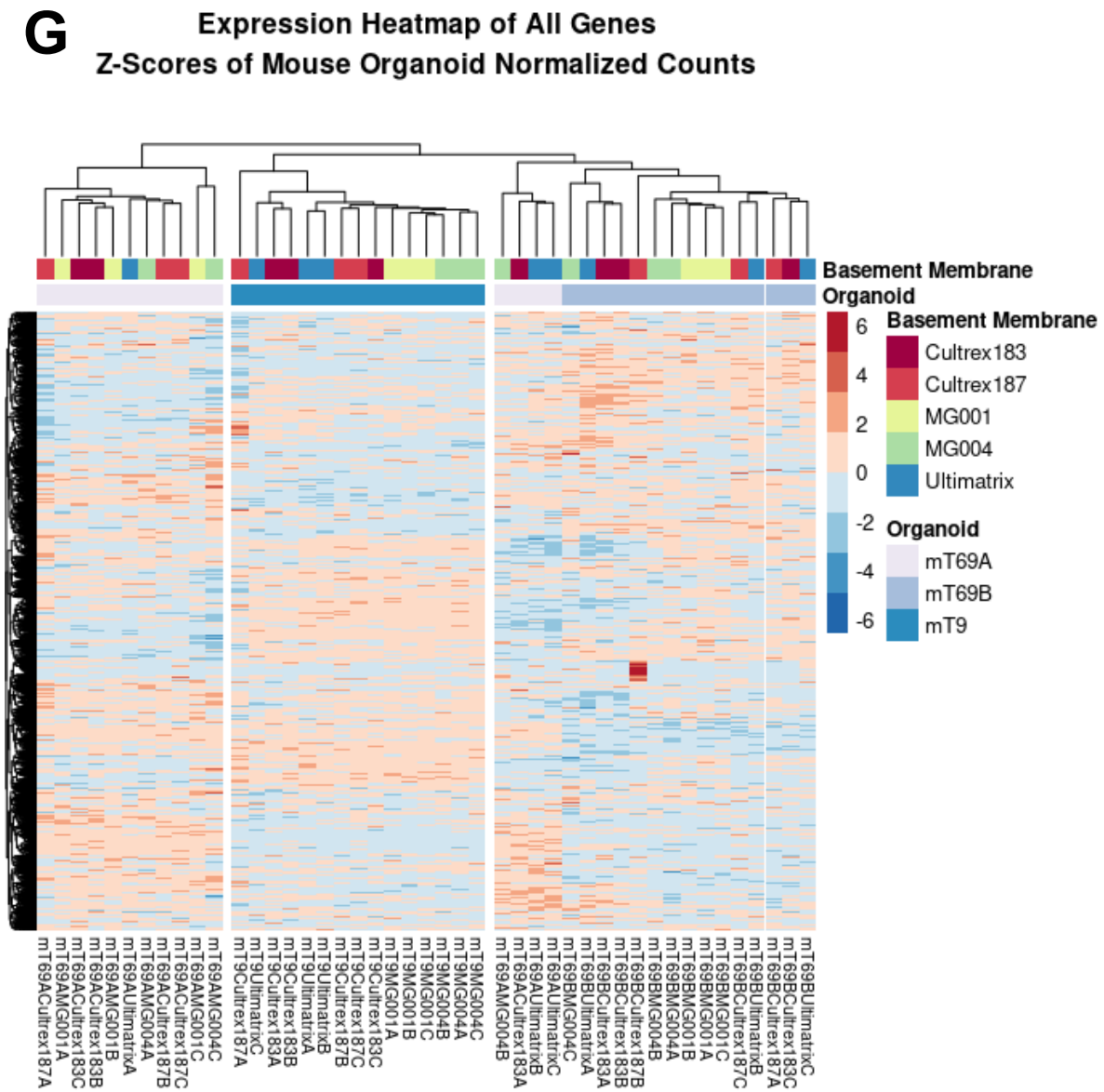

Supplementary Figure 9F-G

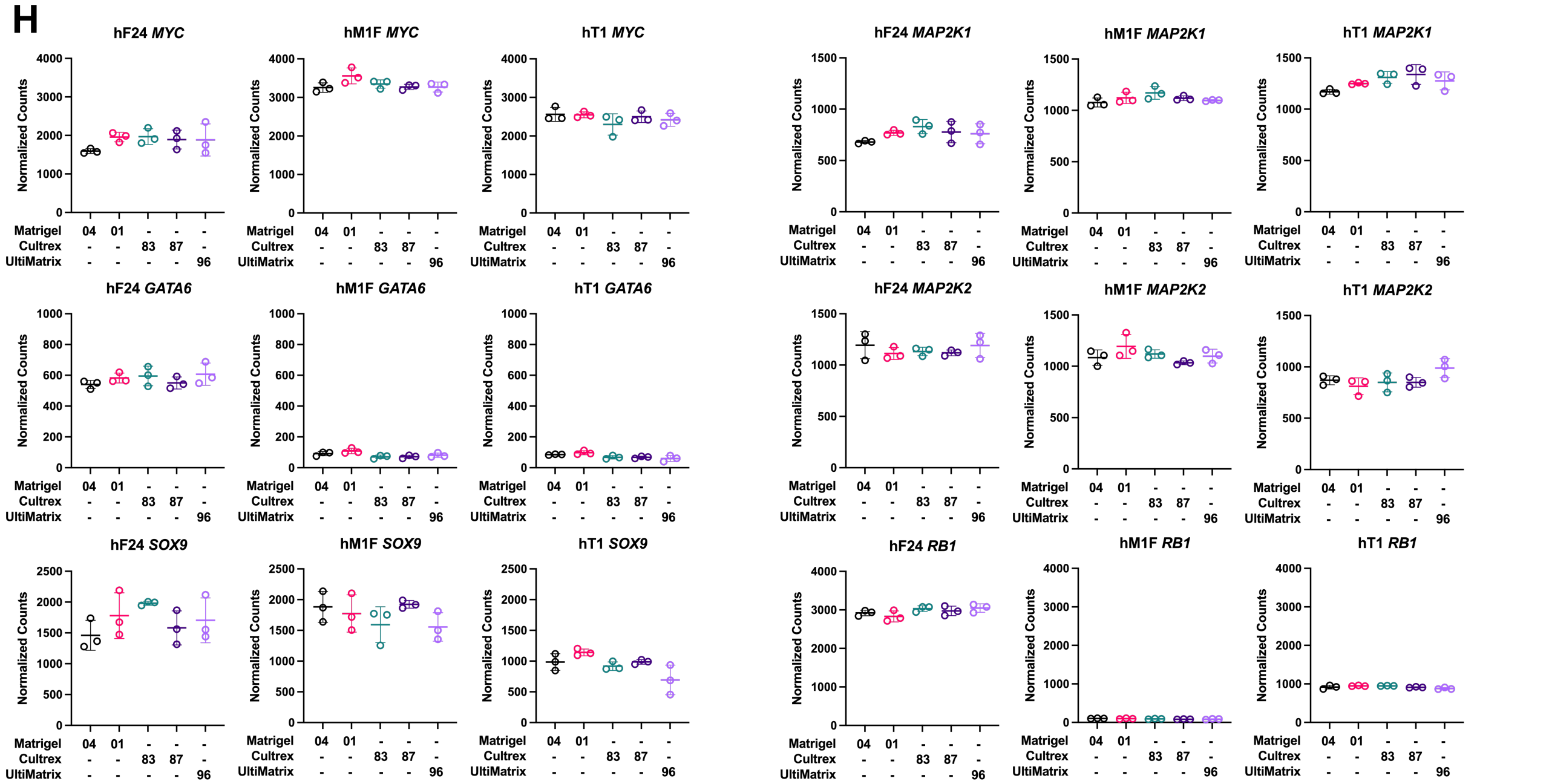

Supplementary Figure 9H

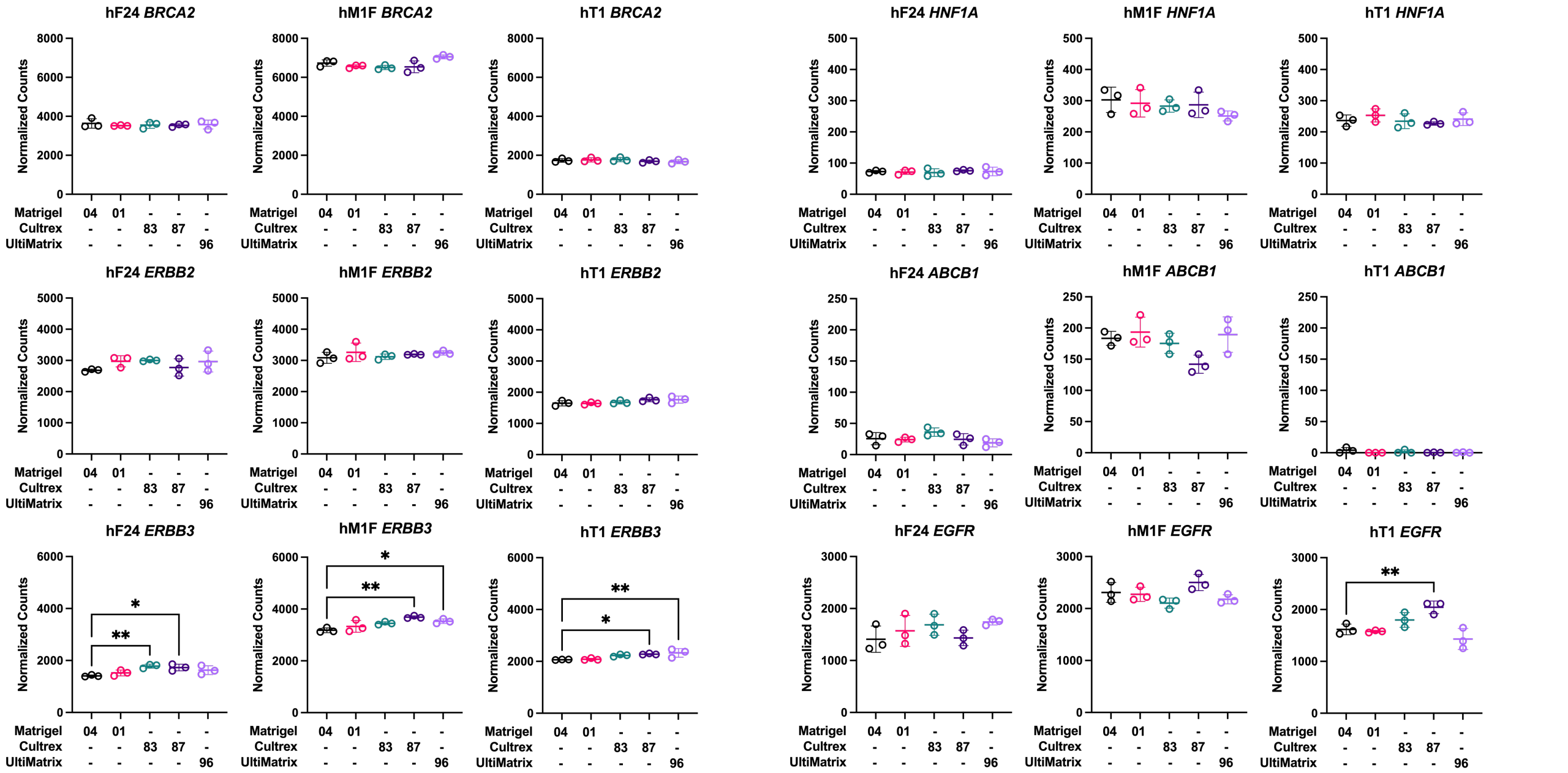

Supplementary Figure 9H